



저작자표시-비영리-변경금지 2.0 대한민국

이용자는 아래의 조건을 따르는 경우에 한하여 자유롭게

- 이 저작물을 복제, 배포, 전송, 전시, 공연 및 방송할 수 있습니다.

다음과 같은 조건을 따라야 합니다:



저작자표시. 귀하는 원저작자를 표시하여야 합니다.



비영리. 귀하는 이 저작물을 영리 목적으로 이용할 수 없습니다.



변경금지. 귀하는 이 저작물을 개작, 변형 또는 가공할 수 없습니다.

- 귀하는, 이 저작물의 재이용이나 배포의 경우, 이 저작물에 적용된 이용허락조건을 명확하게 나타내어야 합니다.
- 저작권자로부터 별도의 허가를 받으면 이러한 조건들은 적용되지 않습니다.

저작권법에 따른 이용자의 권리는 위의 내용에 의하여 영향을 받지 않습니다.

이것은 [이용허락규약\(Legal Code\)](#)을 이해하기 쉽게 요약한 것입니다.

[Disclaimer](#)

이학박사학위논문

Activator and inhibitor of Hepatitis B virus (HBV) capsid assembly

B형 간염 바이러스 캡시드형성에 관여하는 촉진제와 억제제

2018년 12월

서울대학교 대학원

생명과학부

서 현 옥

B형 간염 바이러스 캡시드형성에 관여하는 촉진제와 억제제

Activator and inhibitor of Hepatitis B virus (HBV) capsid assembly

지도교수 : 정 구 흥

이 논문을 이학박사 학위논문으로 제출함


2018년 12월


서울대학교 대학원 생명과학부

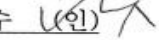
서 현 옥


서현옥의 이학박사 학위논문을 인준함


2018년12월

위 원 장 : 정 용 근 (인) 

부위원장 : 정 구 흥 (인) 

위 원 : 황 덕 수 (인) 

위 원 : 박 동 은 (인) 

위 원 : 유 영 도 (인) 

Activator and inhibitor of Hepatitis B virus (HBV) capsid assembly

**A dissertation submitted in partial
fulfillment of the requirement
for the degree of**

DOCTOR OF PHILOSOPHY

**To the Faculty of
Department of Biological Sciences
At
Seoul National University**

Data Approved:

2018.12


Deog Su Hwang

Deog Su Hwang


Abstract

Activator and inhibitor of Hepatitis B virus (HBV) capsid assembly

Hyun-Wook Seo

Department of Biological Science

The Graduate School

Seoul National University

Hepatitis B virus (HBV) infection is a major risk factor for chronic liver disease, cirrhosis, and hepatocellular carcinoma (HCC) worldwide. While multiple hepatitis B drugs have been developed, build up of drug resistance during treatment or weak efficacies observed in some cases have limited their application. Therefore, there is an urgent need to develop substitutional pharmacological agents for HBV-infected individuals. Here, we identified cetylpyridinium chloride (CPC) as a novel inhibitor of HBV. Using computational docking of CPC to core protein, microscale thermophoresis analysis of CPC binding to viral nucleocapsids, and *in vitro* nucleocapsid formation assays, we found that CPC interacts with dimeric viral nucleocapsid protein (known as core protein or HBcAg). Compared with other HBV inhibitors, such as benzenesulfonamide (BS) and sulfanilamide (SA), CPC achieved significantly better reduction of HBV particle number in HepG2.2.15 cell line, a derivative of human HCC cells that stably

expresses HBV. Taken together, our results show that CPC inhibits capsid assembly and leads to reduced HBV biogenesis. Thus, CPC is an effective pharmacological agent that can reduce HBV particles.

As another finding, Heat shock proteins (Hsps) are important factors in the formation of the HBV capsid and in genome replication during the viral life cycle. Hsp90 is known to promote capsid assembly. However, the functional roles of Hsp70 in HBV capsid assembly with Hsp90 have not been studied so far. Using microscale thermophoresis analyses and *in vitro* nucleocapsid formation assays, we found that Hsp70 bound to a HBV core protein dimer and facilitated HBV capsid assembly. Inhibition of Hsp70 by methylene blue (MB) led to a decrease in capsid assembly. Moreover, Hsp70 inhibition reduced intracellular capsid formation and HBV virus particle number in HepG2.2.15 cells. Furthermore, we examined synergism between Hsp70 and Hsp90 on HBV capsid formation *in vitro*. Our results clarify the role of Hsp70 in HBV capsid formation via an interaction with core dimers and in synergistically promoting capsid assembly with Hsp90.

Keywords : HBV (Hepatitis B virus), Capsid assembly, CPC (Cetylpyridinium chloride), Hsp70 (Heat shock protein 70), Nucleos(t)ide analogues, Synergistic effect, Microscale thermophoresis

Student Number : 2014-21263

TABLE OF CONTENTS

Chapter 1. Overview of the Hepatitis B virus capsid assembly

1. HBV (Hepatitis B virus)	9
2. HBV capsid assembly	11
3. Heat shock proteins (HSPs)	12
4. Nucleos(t)ide analogues	13

Chapter 2. Cetylpyridinium chloride interacting with the Hepatitis B virus core protein inhibits capsid assembly

- Introduction	20
- Materials and Methods	22
- Results	27
- Discussion	31
- Reference	59

Chapter 3. Heat shock protein 70 and Heat shock protein 90 synergistically increase hepatitis B viral capsid assembly

- Introduction	64
- Materials and Methods	65
- Results	69
- Discussion	72
- Reference	83

LIST OF FIGUERS

Chapter 1. Overview of the Hepatitis B virus capsid assembly

- Fig. 1.** Hepatitis B virus life cycle. 15
- Fig. 2.** Hepatitis B virus coding organization and virion structure. 16
- Fig. 3.** Hepatitis B virus capsid and virion structure. 17
- Fig. 4.** Hepatitis B virus replication and capsid assembly inhibitors. 18

Chapter 2. Cetylpyridinium chloride interacting with the Hepatitis B virus core protein inhibits capsid assembly

- Fig. 1.** HBV virion inhibitory effects in 978 FDA approved drugs. 34
- Fig. 2.** In vitro HBV capsid assembly inhibitory effects of first candidate drugs. 36
- Fig. 3.** CPC inhibits HBV capsid assembly *in vitro*. 37
- Fig. 4.** Interaction and conformational change of HBV Cp149 with the novel capsid assembly inhibitor CPC. 38
- Fig. 5.** Interaction of CPC with diverse proteins. 39
- Fig. 6.** Inhibition of HBV capsid assembly by CPC *in vivo*. 40
- Fig. 7.** Relative HBV DNA change by CPC daily treatment duration and concentration. 41
- Fig. 8.** Comparison of HBV DNA inhibition between CPC and other nucleos(t)ide analogues. 42
- Fig. 9.** Comparison of CPC and LDD-3647 as HBV DNA inhibitors. 43

Fig. 10. IC50 values and HBV DNA change for HBV capsid inhibitor and nucleos(t)ide analogues.	44
Fig. 11. Relative pgRNA levels after various drugs treatments in HepG2.2.15 cell.	45
Fig. 12. HepG2.2.15 cell viability in CPC daily treatment in different duration and concentrations.	46
Fig. 13. Comparison of drug cytotoxicity after various drugs treatments in HepG2.2.15.	47
Fig. 14. Comparison of HBV cccDNA level change by treatment concentration between CPC and ENT.	48
Fig. 15. Transmission electron micrographs of untreated and CPC-treated Cp149 capsids.	49
Fig. 16. Numerical interpretation of capsid assembly inhibition.	50
Fig. 17. Numerical interpretation of capsid assembly inhibition for SA and BCM-599.	51
Fig. 18. Antiviral activity of CPC in combinational effect of CPC and LAM.	52
Fig. 19. The graphical representations obtained from the CompuSyn Report and schematic of capsid assembly inhibition.	53

Chapter 3. Heat shock protein 70 and Heat shock protein 90 synergistically increase hepatitis B viral capsid assembly

Fig. 1. Hsp70 promotes HBV core protein assembly.	76
Fig. 2. Synergistic effect between Hsp70 and Hsp90 on HBV capsid assembly.	77

Fig. 3. Comparison of HBV capsid assembly increasing with Hsp70 or Hsp90.	78
Fig. 4. Various combination of Thermophoresis analysis.	79
Fig. 5. Inhibition of Hsp70 and Hsp90 reduce HBV replication in HepG2.2.15 cells.	80

LIST OF TABLES

Chapter 2. Cetylpyridinium chloride interacting with the Hepatitis B virus core protein inhibits capsid assembly

Table 1. ADMET property of HBV inhibitor candidates.	54
Table 2. Capsid particle classification.	55
Table 3. Inhibitor affinity derived in numerical interpretation.	56
Table 4. IC ₅₀ values and CI index of inhibitor CPC-LAM cocktails.	57
Table 5. Equations used in numerical analysis of capsid assembly inhibition.	58

Chapter 3. Heat shock protein 70 and Heat shock protein 90 synergistically increase hepatitis B viral capsid assembly

Table 1. CI values of Hsp70 and Hsp90 combinations on HBV capsid assembly	81
Table 2. Kd values derived from Thermophoresis analysis.	82

LIST OF ABBREVIATIONS

AML	Amlodipine besylate	AMO	Amoxicillin
BS	Benzenesulfonamide	CI	Combination index
CLZ	Clozapine	Cp149	Core protein 149
CPC	Cetylpyridinium chloride	DRI	Dose reduction index
FLU	Fluocinonide	GLI	Gliquidone
GST	Glutathione S-transferase	HBV	Hepatitis B virus
LAM	Lamivudine	RFC	Tetracycline HCl
HCC	Hepatocellular carcinoma	IDO	Idoxuridine
LAM	Lamivudine	MDM2	Mouse double minute 2
MST	Microscale thermophoresis		homolog
RFC	Rofecoxib	SA	Sulfanilamide
TAK1	Transforming growth factor beta-activated kinase 1	TET	Tetracycline HCl
		TPH	Tripelennamine HCl

Chapter 1

Overview of the Hepatitis B virus capsid assembly

1. HBV (Hepatitis B virus)

Hepatitis B virus (HBV) is a member of hepadnaviridae family, a group of DNA viruses cause chronic and acute hepatic infection in diverse of species. Viruses in Hepadnaviridae family infected some birds and mammals including woodchucks (WHV), duck (DHBV) (Beasley, 1988; Lee, 1997). In human, over 240 million people are consistently infected with HBV (Hepatitis B virus) in worldwide, and about 780 thousand people die every year due to hepatitis B virus. Many of the people infected in HBV develops chronic hepatitis, cirrhosis, and hepatocellular carcinoma (HCC) (Waite et al., 1995). HBV infection is occurred through virus containing blood transfusion or sexual contact with infected host. In persistent infections, HBV proliferates through viral replication in host hepatocyte. During 20 to 30 years of viral persistence, chronic HBV patients are at a risk of developing HCC (Beasley et al., 1981).

HBV DNA replication proceeds in not conventional semi-conservative DNA synthesis, but by reverse transcription of an RNA intermediate. Pregenomic RNA (pgRNA) serve as the template for reverse transcription and is produced by host RNA polymerase (Buscher et al., 1985).

In HBV life cycle, virions binds to host membrane receptor and their nucleocapsids are delivered into the host cytoplasm. These nucleocapsid translocate to the nucleus, where viral genomic DNA is converted from relaxed circular DNA (rcDNA) form to covalently closed circular DNA (cccDNA) form. This stage is thought to be activated by hepatocyte DNA polymerase. Then viral mRNA and pgRNA are transcribed from the cccDNA by host RNA

polymerase, transcribed RNA are transported into cytosol where are translated to C (Core), P (Polymerase), S (Surface) and X proteins. Within HBV capsid, viral DNA synthesis is initiated with following minus strand, plus strand synthesis occurs. After completion of viral genomic DNA synthesis, progeny cores bud into host membrane. Finally, enveloped virions are secreted via vesicular transport pathways (Figure 1) (Ganem and Varmus, 1987; Seeger and Mason, 2000).

HBV has a circular, partially double-stranded 3.2kbp DNA that contains four overlapping open reading frames (ORFs). The Core (C) region encodes the HBV nucleocapsid proteins. Polymerase (P) region encodes HBV polymerase that functions in viral genomic replication. Surface (S) region encodes the viral surface glycoprotein and X (X) region encodes the X protein of which the functions are not fully understood (Figure 2) (Lee, 1997). Using transmission electron microscopy (TEM), it is shown that HBV has 42 to 47 nm double-shelled particles called Dane particles. HBV DNA, partially double stranded, is in a relaxed circular (rc) form and the two DNA strands are not symmetric. The plus strand is shorter than the minus strand and both strands have capped oligonucleotide at 5' ends. 5' end of both strands have short (11nt) direct repeats (DRs) regions in the viral DNA (Argos and Fuller, 1988; Budkowska et al., 1977).

2. HBV capsid assembly

HBV capsid is in an icosahedral symmetry, assembled by nucleocapsid proteins which is and surrounded by lipoprotein envelope (Summers, 1988). 120 core protein dimers build a T=4 icosahedral capsid complex which is also found in several other virus species. HBV core protein consists of N-terminal assembly domain (1-149 aa) and C-terminal binding domain (150-183/185aa, protamine domain). The assembly domain interacts with other core protein in icosahedral capsid structures and protamine domain interacts with the pgRNA. Cp149 only contains N-terminal assembly domain and the C-terminal binding domain is truncated. Cp149 is used in in-vitro capsid assembly assay (Figure 3) (Crowther et al., 1994; Selzer et al., 2014). Encapsulation of genomic RNA is the initial step in HBV genomic replication. Reverse transcription occurs in the assembled viral core particles. Encapsidated pregenomic RNA in capsid particles indicated that the pgRNA can serve as a template for reverse transcription. Core protein is required to form the packaging structure, and capsid assembly proceeds through core protein dimer interactions.

In addition to core protein, polymerase gene is necessary for RNA packaging. Polymerase of viral RNA packaging is different from the case in retrovirus. The stem-loop of ϵ element is conserved among all hepadnavirus that has major functions to Polymerase-RNA interaction (Summers and Mason, 1982).

Capsid assembly inhibition has advantageous in various HBV drug resistant mutation compared

to the polymerase inhibition. Recent studies focus on heterocyclic compounds that target HBV capsid assembly. These compounds are safer and more effective as anti-viral drugs (Seeger and Mason, 2000).

3. Heat shock proteins (HSPs)

Heat shock proteins (HSPs) have been conserved and existed in prokaryote and eukaryote organisms. HSPs are found in many cellular compartments and play an important role in protein homeostasis . Many factors such as toxic materials, heat or metal stimulus in cells provoke stress related protein formation. In muscle cells, HSP levels are elevated by increase of cellular stress. Increased HSPs cause gene expression changes. Internal and external conditions are triggered in cellular stress. Cells exposed by heat begin producing stress proteins, heat shock proteins (HSPs) (Whitley et al., 1999). HSPs have chaperone functions. There are diverse functions in chaperone proteins (Nahleh et al., 2012). 1) Chaperones function in cell homeostasis and cellular response to stress. 2) They prevent protein aggregation by folding and unfolding process. 3) They affect protein kinetics and productions. 4) They regulate in cell signal transductions.

As a chaperone, HSPs are found in many living organisms. HSPs are synthesized in response to diverse stress including heat, cold temperature, viral infections and UV radiation. HSP genes are expressed during cell growth. HSPs bind to unfolded or denatured proteins and aid their folding

to right functions. HSPs are involved in every cellular process associated with cell growth, DNA synthesis, transcription, translation, and protein transport. In immune systems, HSPs significantly influence immune response (Mager and Ferreira, 1993; Mathew and Morimoto, 1998).

HSPs were classified by their molecular weight, for example Hsp90 (85-90 kDa), Hsp70 (65-70 kDa), Hsp60, Hsp20 and so on (Whitley et al., 1999). Our experimental results focused on Hsp70 and Hsp90. Hsp70 is essential in protein translocation, synthesis, storage, and is found in diverse cellular compartments (nucleus, mitochondria and so on) (Alderson et al., 2016; Flaherty et al., 1990). Hsp90 plays an important role in steroid receptor complexes. Hsp90 acts on many other proteins in their stabilizations in malignant transformation of cells. In tumor cells, activated Hsp90 affects cell proliferation and apoptosis. Hsp90 is one of the most abundant protein in eukaryotes and is essential in *Drosophila melanogaster* and yeast. Hsp90 plays an important role in regulation of signaling molecule and contributes to homeostasis under cellular stress conditions. Hsp90 has two isoforms; Hsp90 α and Hsp90 β are differentially expressed in multicellular organisms (Pratt, 1997; Young et al., 2001).

4. Nucleos(t)ide analogues

There are available drugs against HBV approved by FDA, such as lamivudine, adefovir dipivoxil, telbivudine, entecavir and tenofovir disoproxil fumarate (Grimm et al., 2011). These

nucleos(t)ide analogues target the HBV polymerase. Recent accepted treatments for chronic hepatitis B use nucleos(t)ide analogues such as lamivudine or adefovir (Figure 4). However, long-term use of lamivudine causes viral resistance, resistance mutation and overdose of drugs (Mutimer et al., 2000). Currently diverse nucleos(t)ide analogues are being developed with some of them tested at the early clinical trials. Combining individual drugs may produce synergistic HBV anti-viral effects (Korba, 1996). Nucleos(t)ide analogues exert anti-viral effect through integration into HBV DNA, which induces termination of synthesis. Effective drugs should show high affinity to viral polymerase and incorporate into the viral DNA. However therapeutic safety issue arises when drug affinity for host polymerase causes integration in mitochondria DNA or host DNA and induces drug-related toxicity (Wolters et al., 2001).

Modern treatment of HBV involves combinational use of different anti-viral drugs, because it has been shown to reduce the drugs resistance. Further studies needed to lower the level of HBV replication, drugs resistance or side effects.

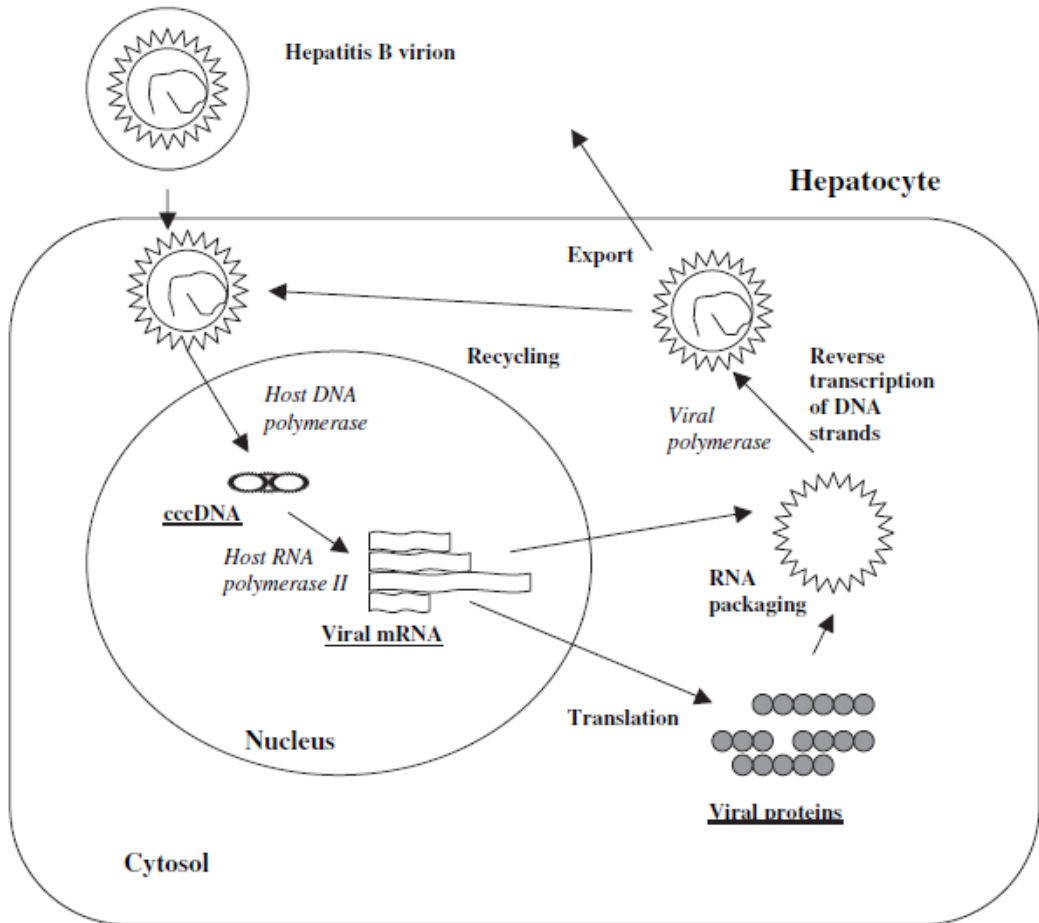


Figure 1. Hepatitis B virus life cycle.

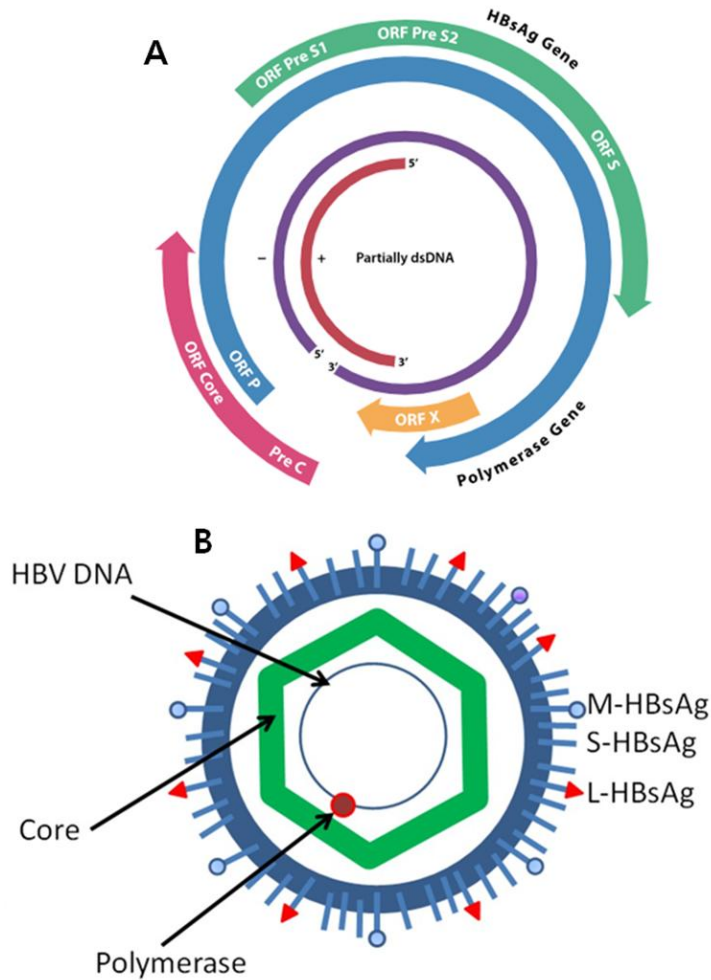


Figure 2. Hepatitis B virus coding organization and virion structure.

A. Inner circle represent virion DNA, positive and negative strands consist of partial double strand DNA. Outer circle represent four ORF that X, P (Polymerase), C (Core), S (Surface). B. Surface proteins consist of L(large), M(middle), S(small)-HBsAg. Icosahedral capsid constructed by core protein dimer subunits. HBV DNA and polymerase existed in capsid particle.

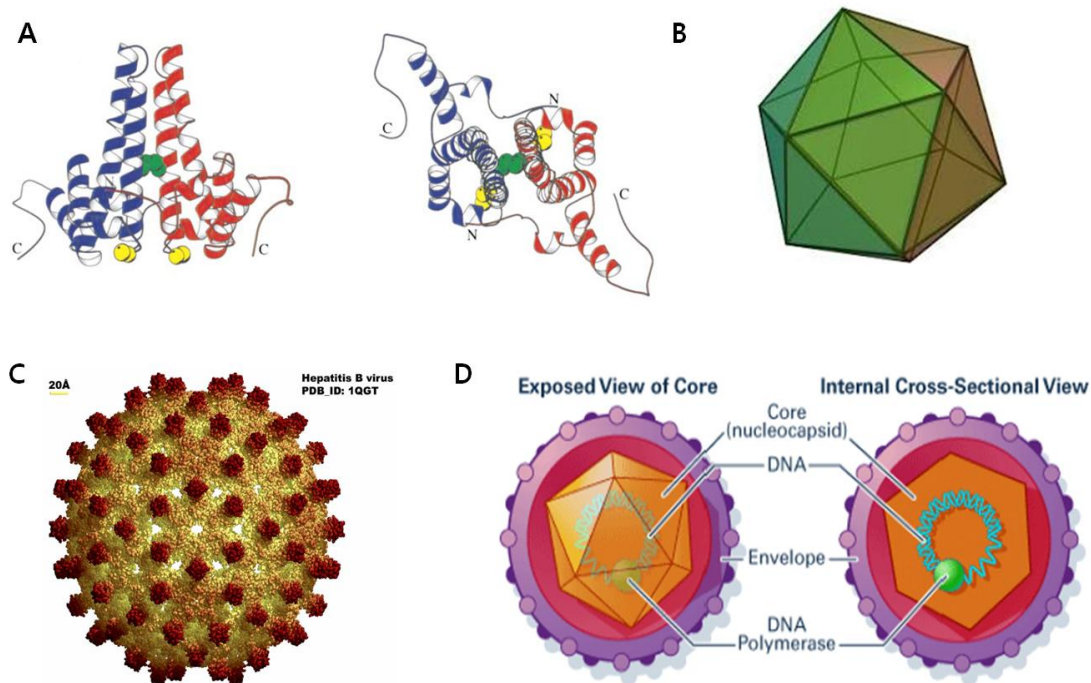


Figure 3. Hepatitis B virus capsid and virion structure.

A. HBV core protein dimer structure. Each monomer (17kDa) binds by disulfide bond. left is lateral view and right is top view. B. Icosahedral capsid structure. HBV capsid was constructed by 180 number of core dimer subunits ($T=3$). C. Virion image made by computer modeling. D. Exposed (left) and internal (right) cross-sectional view of HBV virion.

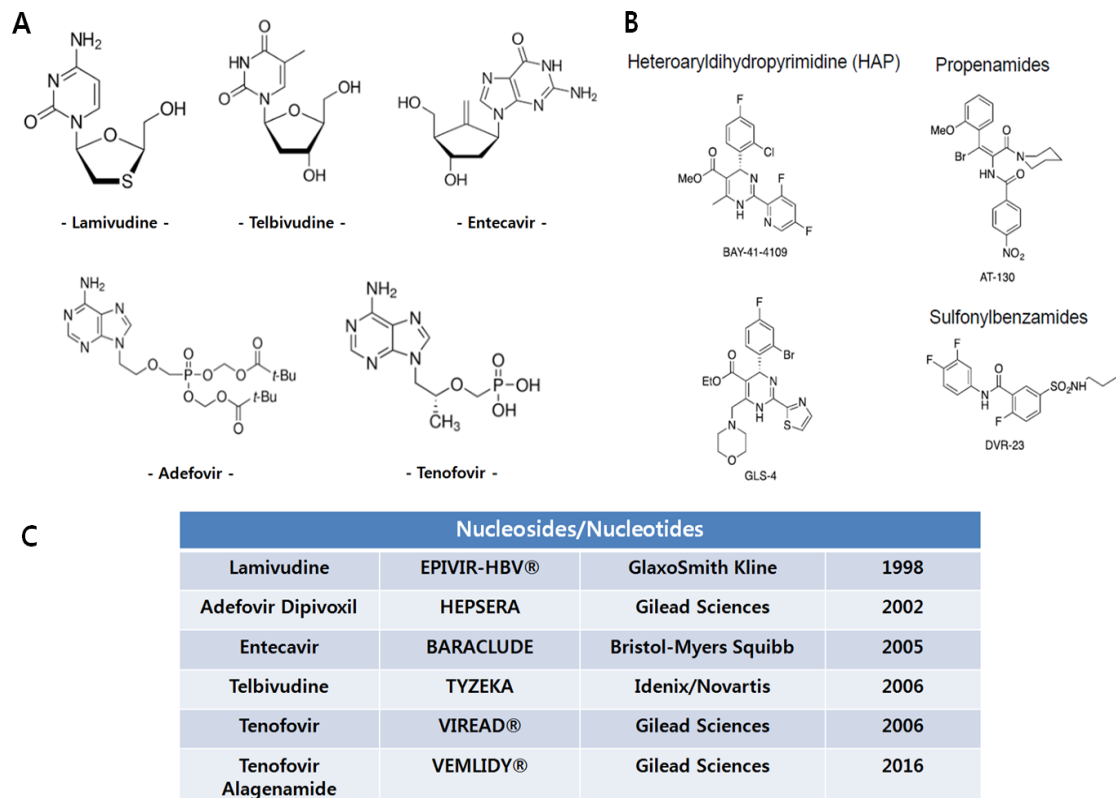


Figure 4. Hepatitis B virus replication and capsid assembly inhibitors.

A. Nucleos(t)ide analogues that approved by FDA. B. HBV capsid assembly inhibitors. C. FDA approved drugs for HBV replication inhibition (drugs name, drugs company, approved years).

Chapter 2

Cetylpyridinium chloride interacting with the Hepatitis B

virus core protein inhibits capsid assembly

Introduction

Hepatitis B virus (HBV) causes chronic hepatitis, and the number of infections is rapidly increasing each year (Ott et al., 2012; Zuckerman, 1999b). Chronic HBV infection is closely associated with the development of cirrhosis and hepatocellular carcinoma (HCC) (Paradis, 2013). The partially double-stranded DNA genome of HBV is 3.2 kb in size, and encodes 4 distinct proteins: core protein, surface protein (large, middle, small), X protein, and a polymerase capable of both DNA-dependent and RNA-dependent DNA polymerization (Seeger and Mason, 2000). During the course of infection, the HBV genome is transformed into covalently closed circular DNA (cccDNA) with the aid of the nucleus repair system (Seeger and Mason, 2000). The cccDNA then serves as a template for transcription of pregenomic RNA (pgRNA) by the host's RNA polymerase (Seeger and Mason, 2000). HBcAg can be assembled into T=3 or T=4 icosahedral capsid structures, and an envelope is formed from insertion of surface antigens into the host intracellular membrane (Seeger and Mason, 2000).

HBV has been researched by biologists and pharmacologists, and multiple therapeutics have been developed to inhibit viral replication (Stein and Loomba, 2009). For example, lamivudine (LAM) and adefovir were introduced as HBV replication inhibitors, and were administered to treat HBV infections. These nucleos(t)ide analogue drugs usually induce drug resistance and show low efficacy (Doong et al., 1991b). While the recently developed entecavir and telbivudine demonstrated less drug resistance, insufficient studies on these drugs were

conducted; results indicated that they vary in efficiency between patients, and induce other mutant resistance as a side effect (Pan et al., 2017). Thus, previous treatment regimens for these HBV replicative inhibitor drugs involved diverse combinatorial administration depending on an individual's susceptibility to each drug species (Brunetto and Lok, 2010). Therefore, there is increased attention and demand for new drugs that target different parts of the HBV infection process. One potential mechanism of action is to inhibit capsid assembly, which in turn inhibits replication and build up of virus particles (Vanlandschoot et al., 2003).

Our research focused on targeting the HBV capsid; the core protein has 183-185 amino acids with two functional domains (Hirsch et al., 1990). Assembly domain (1-149 aa) interacts with neighboring core proteins to form the icosahedral capsid structure, while protamine domain (150-183/185 aa) interacts with pgRNA to regulate reverse transcriptase (RTs) activity (Hirsch et al., 1990; Wynne et al., 1999). To determine its exact effect on *in vitro* capsid assembly, we used a C-terminal region truncated, assembly domain of the core protein; Cp149. Cp149 form dimers and three dimers assemble into a hexamer structure. The Cp149 hexamer acts as a nucleus and stabilizes capsid assembly (Lott et al., 2000).

In a previous study, cetylpyridinium chloride (CPC) was shown to possess anti-bacterial activity (Popkin et al., 2017). Nevertheless, the inhibitory effect of CPC against Hepatitis B virus remains to be elucidated. Capsid inhibitors such as benzenesulfonamide (BS) and sulfanilamide (SA) inhibit HBV capsid assembly at relatively high half maximal inhibitory

concentrations (IC_{50} ; 7–200 μ M) (Cho et al., 2014; Cho et al., 2013). In this paper, we found that CPC interfered with HBV capsid assembly with a low IC_{50} (2–3 μ M). We aimed to determine the functional role of CPC in HBV capsid assembly and demonstrated that CPC significantly decreased HBV biogenesis through binding to dimeric core proteins, in consequence, preventing capsid formation.

Materials and Methods

Purification of Cp149, HBV capsid assembly analysis, and sucrose density gradient analysis

Cp149 was cloned directly using a pET28b vector (Novagen, Madison, USA). Constructs were transformed into BL21(DE3) + pLysS *Escherichia coli* (Novagen, Madison, USA). Cp149 was induced by 1 mM isopropyl- β -D-thiogalactopyranoside (IPTG) and incubated at 37°C for 4 h. Cp149 dimers were stored in stock solution (100 mM glycine (pH 9.5), 10% glycerol) at -70°C. Capsid assembly reaction was conducted in assembly reaction buffer (50 mM HEPES, 15 mM NaCl, 10 mM $CaCl_2$ (pH 7.5)) with candidate drug concentration (ranging from 1-20 μ M) at 37°C for 1 h. Assembled particles were detected by immunoblot analysis using mouse monoclonal anti-HBV core antibody (Abcam, Cambridge, UK) (Kim et al., 2015). Sucrose density gradient analysis was conducted by ultracentrifugation (HITACHI, Tokyo, Japan) for 3.5

h at 250,000 g. Samples were prepared after CPC (20 μ M) and SA (200 μ M) treatments.

Fractions of sucrose concentrations were analyzed by 15% SDS-PAGE followed by immunoblot analysis using mouse monoclonal anti-HBV core antibody (Abcam, Cambridge, UK) (Kang et al., 2006).

Measurement of cell viability

Cell viability was determined by the 3-(4,5-dimethylthiazol-2-yl)-2,5-diphenyltetrazolium bromide (MTT) assay. HepG2.2.15 cells were cultured at 80% confluency in 96-well plates and maintained in Dulbecco's modified Eagle's medium (DMEM, Wellgene, Gyeongsan-si, South Korea). The cells were treated with varying concentrations 0 to 1 μ M of CPC for 24 h and then washed with PBS and treated with the MTT solution for 4 h at 37°C. Absorbance at 570 nm was measured using a microphotometer reader (BioTek, Vermont, USA). Also CPC daily (0-4day) treated and other nucleoside analogues treated samples were measured (Lee et al., 2013).

Protein–small molecule interaction analysis using microscale thermophoresis

Cp149 was labeled with Monolith NT.115 protein labeling kit RED (Nanotemper, Munich, Germany), and was eluted to 10 μ g in the MST buffer (50 mM Tris-HCl (pH 7.4), 150 mM NaCl, 10 mM MgCl₂, and 0.05% Tween-20). CPC was serially diluted (0.02 to 100 μ M) into Cp149 solutions. Samples were incubated at 37°C for 10 minutes, and were analyzed using the

Monolith NT.115 program (Nanotemper, Munich, Germany). All the experiments were performed thrice and analyzed as previously described (Timofeeva et al., 2012).

Quantification of intracellular and extracellular viral DNA by real-time PCR

HepG2.2.15 cells (1 μ M) were treated with 978 FDA-approved chemicals (Cat. L1300, Selleckchem, Houston, USA). Following 24 h incubation, HBV DNA was extracted from the cell and media, and was analyzed by real-time PCR. Total viral DNA was measured using quantitative PCR, the forward primer sequence was 5'-TCCTCTTCATCCTGCTGCTATG-3', and reverse primer sequence was 5'-CGTGCTGGTAGTTGATGTTTCCT-3'. CPC daily (0-5day) treated and other nucleoside analogues treated samples were quantified using realtime PCR (Garson et al., 2005; Shim et al., 2011).

CPC and LAM combination analysis using Compusyn

To evaluate CPC and LAM synergism, we treated HepG2.2.15 cells grown in 96-well plates with CPC and LAM in various ratios (12:1 to 0.33:1). After 24 h, the medium was collected and the concentration of the released HBV particles was measured. IC₅₀ and combination-index (CI) values were calculated using Compusyn (Molecular Pharmacology and Chemistry program, New York, USA). Single drug treatments and combination drug treatment dose-effect curves were fitted into logarithmic functions converging toward the discrete upper bounds in fractional

effect value. IC_{50} values were obtained from the dose-effect curves. Dose reduction index (DRI) was calculated as the ratio of input dose in combinatorial treatment and corresponding single treatment dose in account with equal effect value. CI was calculated by adding the reciprocal value of each DRI for indicating synergism ($CI > 1$, antagonistic effect; $CI = 1$, additive effect; $CI < 1$, synergistic effect) (Chou, 2006, 2010b).

Numerical analysis of capsid assembly inhibition

Based on the molecular simulation, searching for the difference in solvent accessibility between the protomer and free dimeric core protein, we identified the binding sites of contiguous protomers and CPC on the dimeric core protein, Cp149₂. Assembly inhibition was summarized into a competing equilibrium between CPC binding and capsid assembly (Table 5 Eq. 1, 2). Calculations of association constants K_{capsid} and K_{CPC} were based on the equilibria and mass-conservation law (Table 5 Eq. 3, 4). The equilibrium between Cp149₂ and capsid is represented by, K_{capsid} (Table 5 Eq. 5). Equations were recast in terms of capsid and CPC bound Cp149₂ concentrations (Table 5 Eq. 6, 7). The approach in calculating K_{capsid} using a 120th power multivariate function would yield consistent results for free dimer concentration in approximation. Consequently, capsid and CPC bound dimer concentrations is expressed to be linearly and inversely proportional to each other. $[Cp149_2]_{Total}$ and $[CPC]_{Total}$ are already known and values for $[Capsid]$ and K_{capsid} were determined experimentally (Zlotnick et al.,

2002). Capsid assembly detected by immunoblot was interpreted, postulating the absence of protomer oligomers other than the capsid. The CPC association constant was calculated and the inhibition curve was plotted with extrapolated prediction curve. Microscale thermophoresis was interpreted based on the superpositional expression of normalized fluorescence (Table 5 Eq. 8). The Soret coefficient was approximated for capsid particle in terms of Cp149₂ soret coefficient, based on geometrical symmetry and solvent accessibility calculation. Capsid structure was modeled into a spherical symmetric geometry for area calculation and virtual mole fraction coefficient of the capsid. Optimal Soret coefficients and assembly inhibitor association constants were found using the bisection method up to two significant digits. A thermophoretic curve was computed and CPC association constant was obtained (Baaske et al., 2010).

Circular dichroism (CD) analysis

CD analysis was carried out with J-815 (Jasco, Oklahoma City, USA). Spectra were measured using 1 nm bandwidth, scan speed 50 nm/min, response time of 1 s and three accumulations. The CD measurements were made using a quartz cuvette with a 1 cm path length and total protein concentration of 0.1 mg/mL. Values were measured by Spectra manager and Spectra analysis version 2.01A program (Zlotnick et al., 2002).

Transmission electron microscopy (TEM)

For negative staining, 10 μL of assembled Cp149 samples were applied to each carbon-coated grid, and were incubated for 1 min; the grid was stained with 2% uranyl acetate. TEM was conducted on a LIBRA 120 (Carl Zeiss, Oberkochen, Germany) operating at 120 KV at the NICEM (National Instrumentation Center for Environmental Management, Seoul, South Korea). Capsid particles were counted, and classified into three categories: normal, broken, or aberrant capsid. Broken capsid was defined as a spherical, capsid-like structure that is partially broken. Aberrant capsid was defined as a particle that has detectable size (Kang et al., 2006).

Results

1. Capsid assembly assay revealed that CPC is a potent drug for abolishing HBV

HepG2.2.15 cells were treated with FDA-approved chemicals (Figure 1). Out of the 978 chemicals approved by the FDA, 100 chemicals that induced the greatest reduction in viral particles, as assessed by real-time PCR, were selected as first candidates. First candidates were tested for HBV capsid assembly inhibition (Figure 2), and top 10 candidates were selected for further analysis (Figure 3A, Table 1). The HBV core protein Cp149 was treated with 6 out of the 10 chemicals, including CPC (0- 20 μM) (Figure 3B-3G). Among the 6 candidates, CPC showed the most effective capsid assembly inhibition with an IC_{50} of $2.5 \pm 0.5 \mu\text{M}$ while other candidates (AMO, TPH, FLU, GLI, TET) showed IC_{50} greater than 5 μM (Figure 3B-3G). CPC was more effective in inhibiting HBV viral replication than other drug candidates (Figure 3H).

These data suggested that CPC is effective in blocking HBV capsid assembly.

2. CPC interacted and induced conformational change in the HBV Cp149 dimer

The monolith assay is based on thermodynamic changes that denote interactions between proteins and small molecules (Timofeeva et al., 2012). Results indicated that CPC interacts with the HBV Cp149 dimer (Figure 4A). Anti-HBcAg antibodies (Smith et al., 2012) and DMSO were used as positive and negative controls, respectively (Figure 4B, 4C). CPC showed interaction propensity, unlike DMSO (Figure 4). Automatically calculated dissociation constants for 1:1 stoichiometric 1st order reactions were 9.9776 and 2.2998 for CPC and anti-HBcAg antibody, respectively. Dissociation constant for DMSO was undefined, indicating that DMSO doesn't interact with the Cp149 dimer (Figure 4). Also CPC interacts Cp149 dimer, however didn't show interaction with other proteins such as enzyme or antibodies (Figure 5). It means CPC selectively interacts to Cp149 dimer (Figure 5B).

CD was measured for the core protein. DMSO treated core protein did not show significant alterations in molar ellipticity, while core protein treated with BS, a positive control, did. Also, CPC-treated core protein showed a propensity for alteration, indicating that analogous conformational changes are induced in the secondary structure (Figure 4D).

3. CPC suppressed HBV biogenesis by interfering with capsid assembly

We performed sucrose density analysis using Cp149 and CPC. CPC markedly decreased the

amount of capsid (Figure 6A). Next, we determined the *in vivo* activity of CPC using HepG2.2.15 cells (Figure 6B, 6C), since HepG2.2.15 cells release HBV virus particles. CPC inhibited HBV biogenesis in HepG2.2.15 cells; both intracellular and extracellular HBV particles were significantly reduced (Figure 6B). HepG2.2.15 cells showed consistent cell viability when treated with CPC concentrations between 0 to 1 μ M (Figure 6C). We measured extracellular HBV particles to confirm the inhibitory effect of CPC in daily (0-5day) treatments (Figure 7). Also we compared HBV inhibitory effect of CPC with other nucleos(t)ide analogues (Figure 8) and a new HBV capsid assembly inhibitor candidate LDD-3647 (Figure 9) in HepG2.2.15 cells. IC₅₀ values of experimented drugs were measured (Figure 10). CPC showed effective HBV inhibitory effect. Equivalent amounts of pgRNA were measured in the control group of HepG2.2.15 cells and cells treated with CPC (Figure 11A). Meanwhile, other HBV capsid assembly inhibitors exhibited decrease in pgRNA levels at high (1 μ M) concentrations (Figure 11B, 11C). We measured equivalent cell viability levels in different CPC treatment duration (0-4day) and treatment concentration (0-1 μ M) (Figure 12A-12D). The results indicated that CPC didn't show cell cytotoxicity in HepG2.2.15 cells. Also we compared cell viability in HepG2.2.15 cells between nucleos(t)ide analogues and other capsid assembly inhibitors (Figure 13A-13D). We also confirmed cccDNA levels by measuring extracted HBV cccDNA using PCR (Figure 14A). HBV cccDNA levels were consistent in different CPC concentration (0-1 μ M) (Figure 14B).

TEM images also showed that capsid assembly inhibition was induced by CPC (Figure 15). TEM images of capsid assembly with no treatment displayed that circular particles with diameters of 30-35 nm were detected, and resembled bright rings with dark centers (Figure 15B, 15C). However, CPC decreased capsid formation; capsid particles exhibited ruptures and asymmetric modifications (Figure 15D, 15E, Table 2).

4. Numerical illustration of CPC arisen constrain on capsid assembly

In the HBV capsid structure, a dimeric core protein subunit binds to 4 adjacent dimer core protein subunits (Wynne et al., 1999). Inhibitor association constants K_i for CPC, SA and BCM-599 were calculated from the capsid assembly results (Figure 16, 17) (Cho et al., 2014). The capsid assembly inhibition was plotted with the prediction curve, which was extrapolated with the CPC association constant (Figure 16A, Table 5). Microscale thermophoresis data was analyzed and plotted with the computed thermophoresis curve (Figure 16B, Table 5). The CPC binding association constant was calculated to be $1.0 \pm 0.5 \mu\text{M}^{-1}$ in capsid assembly, while in the monolith assay, the optimal association constant was $1.2 \pm 0.9 \mu\text{M}^{-1}$ (Figure 16). SA and BCM-599 showed weaker associations compared to CPC (Figure 17, Table 3).

5. Combination of CPC and LAM shows synergistic effect

LAM reduced secreted virion concentration in HepG2.2.15 cells (Figure 18A). When treated

with both CPC and LAM, HBV virion concentration decreased more compared to single treatments of CPC and LAM alone (Figure 18B). To determine whether treatment of both CPC and LAM reduced the HBV viral concentration synergistically, we calculated CI values using a dose-effect curve (Figure 19A), a combination of index plot (Figure 19B), and an isobologram (Figure 19C) marked by CPC, LAM, and Mix (CPC+LAM). As a result, we confirmed that the virion concentration was reduced synergistically because of CPC and LAM treatment (Figure 18B, 19). In particular, 0.142 μ M CPC with 0.012 μ M LAM, and 0.112 μ M CPC with 0.028 μ M LAM showed strong synergistic effects (Table 4).

These results demonstrate that CPC represses HBV biogenesis by inhibiting the conversion of dimeric Cp149 to capsid structures through receptor ligand interaction with free dimeric subunits (Figure 19D). Together, these findings indicate that CPC is a potent drug for abolishing HBV.

Discussion

Nucleos(t)ide analogues such as adefovir, tenofovir, and entecavir have been used for treating patients with HBV-related liver diseases (Fabrizi et al., 2004). These drugs target RTs, however, RT-targeting drugs have low efficiency, which leads to increasingly high drug dose and drug resistance (Fabrizi et al., 2004). Therefore, new potent antiviral compounds capable of inhibiting viral proliferation through distinct mechanisms are highly desired (Dawood et al.,

2017). We tested HBV capsid assembly inhibitors for selection of novel drug compound. The viral life cycle of HBV, including virion maturation and genome duplication, is highly dependent on capsid assembly (Yang and Lu, 2017). Accordingly, capsid assembly inhibition is a good antiviral target for HBV treatment to effectively suppress HBV infection (Ren et al., 2017). Thus, in this study, we focused on searching for potential drug compound that inhibits HBV capsid assembly. Among the 978 FDA-approved drug compounds (Cat.L1300, Selleckchem, Houston, USA), we selected CPC as an effective candidate that reduces viral replication. CPC inhibited capsid assembly *in vitro*. CPC also showed an insignificant impact on cell viability (up to 1 μ M) while reducing the number of virus particles in HepG2.2.15 cells that release HBV virus (Figures 6B, 6C). It can be deduced that CPC is an effective anti-HBV capsid assembly inhibitor.

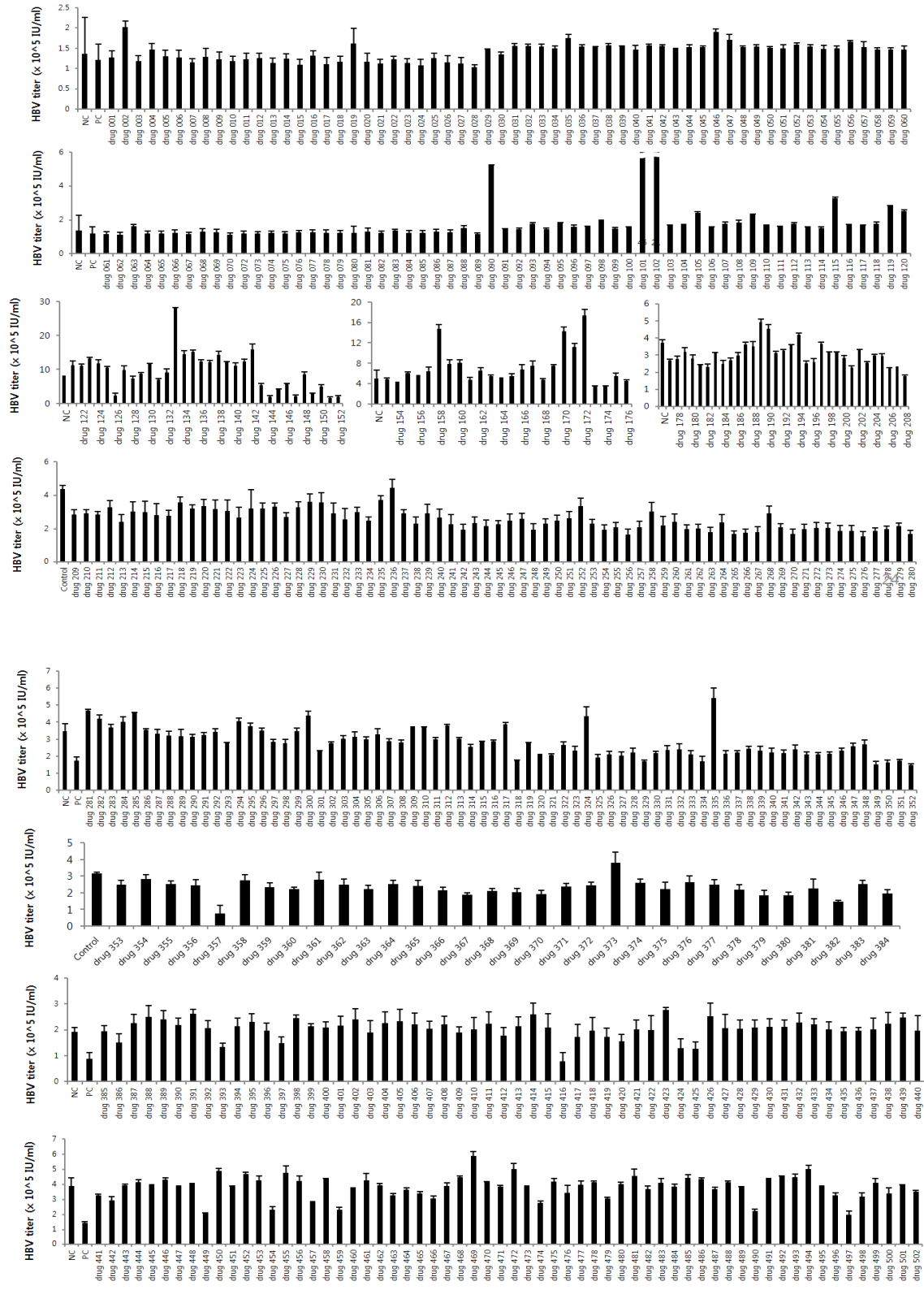
CPC functions as an antiseptic that kills bacteria and other organisms (Lee et al., 2017). It has also been widely used in pesticides and mouthwashes (Lee et al., 2017). According to the ADMET data, CPC had low penetration and absorption due to its high hydrophobicity and low polar surface area, which are disadvantageous for drug delivery (Table 1). For use in clinical settings, a sufficient plasma concentration must be achieved. Therefore, we propose supplements that can help penetrate cells to maximize the inhibitory effect of CPC.

There are several nucleos(t)ide analogues, including LAM, that target HBV-RT (Stein and Loomba, 2009). We showed a synergistic effect on HBV replicative inhibition in HepG2.2.15

cell when treated with both LAM and the capsid assembly inhibitor CPC (Figure 18B).

Similarly, our previous study reported that the capsid assembly inhibitor BCM-599 also showed a synergistic effect when treated with LAM. Together, these results indicated effective HBV viral biogenesis inhibition induced by co-treatment with nucleos(t)ide analogue drugs and capsid assembly inhibitors.

Here, we identified CPC as a novel HBV inhibitor with *in vivo* and *in vitro* systems and demonstrated that CPC induces HBV inhibition through inhibition of viral capsid assembly. These effects were confirmed by TEM. Overall, our findings contribute to the development of effective inhibitors against HBV biogenesis.



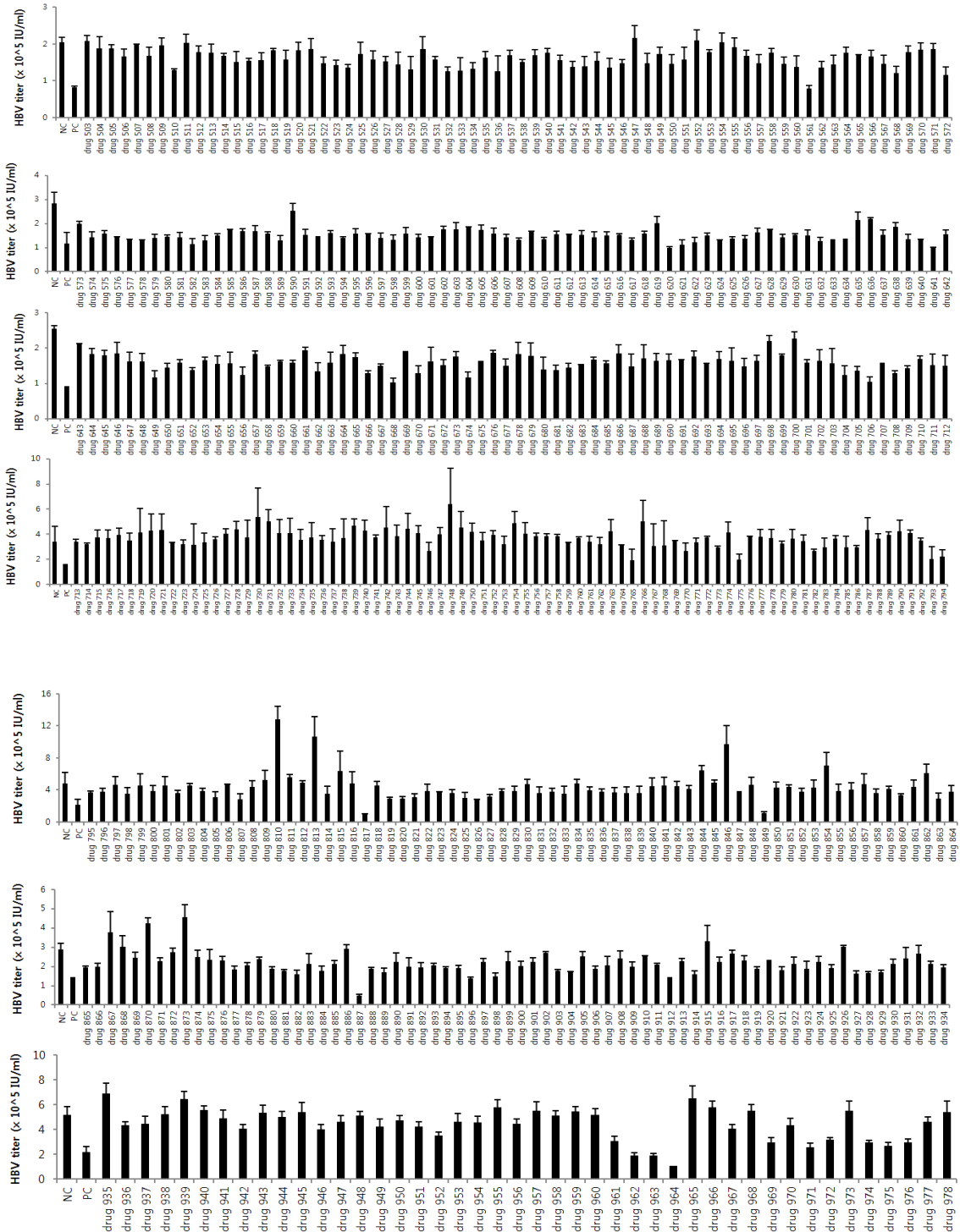


Figure 1. HBV virion inhibitory effects in 978 FDA approved drugs.

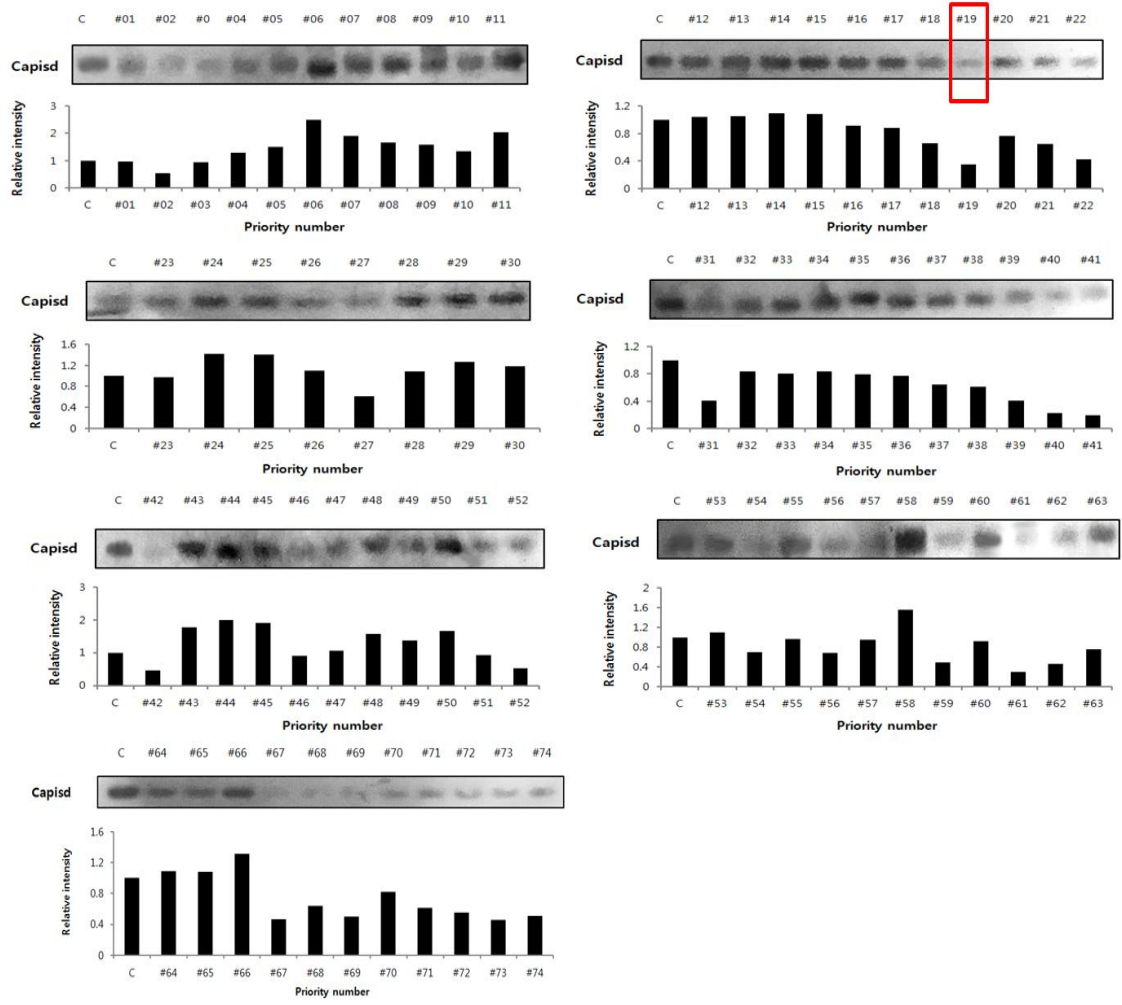


Figure 2. In vitro HBV capsid assembly inhibitory effects of first candidate drugs. Red mark indicate Cetylpyridinium chloride which is selected as an HBV capsid assembly inhibitor candidate.

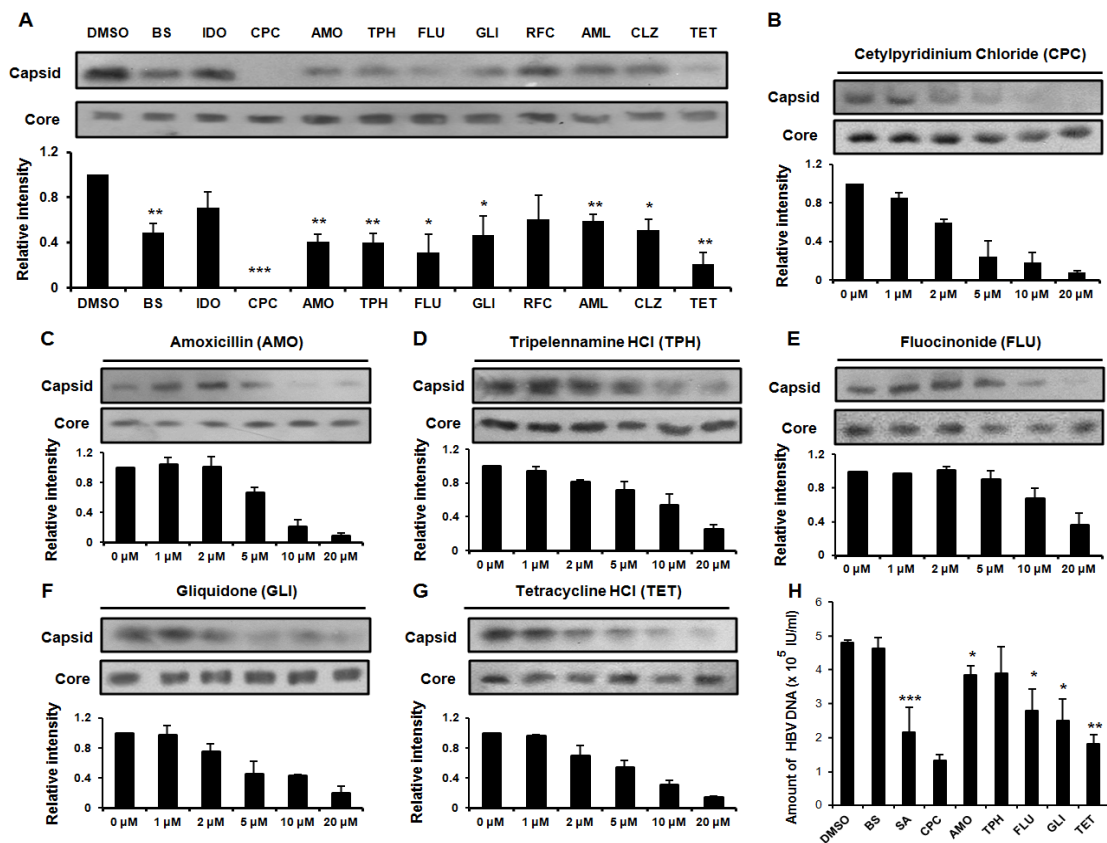


Figure 3. CPC inhibits HBV capsid assembly *in vitro*.

A. Capsid assembly assay with HBV Cp149 and candidates for inhibiting HBV capsid assembly.

B-G. Capsid assembly assay using HBV capsid inhibitor candidates (0-20 μM). IC₅₀ of CPC

was measured as an average of the immunoblot band intensity. H. Quantitation of HBV DNA

following treatment with 1 μM core assembly inhibitors. Values are mean ± standard error of the

mean (SEM, n = 4 per group); **p* < 0.05, ***p* < 0.01, and ****p* < 0.001, *t* test.

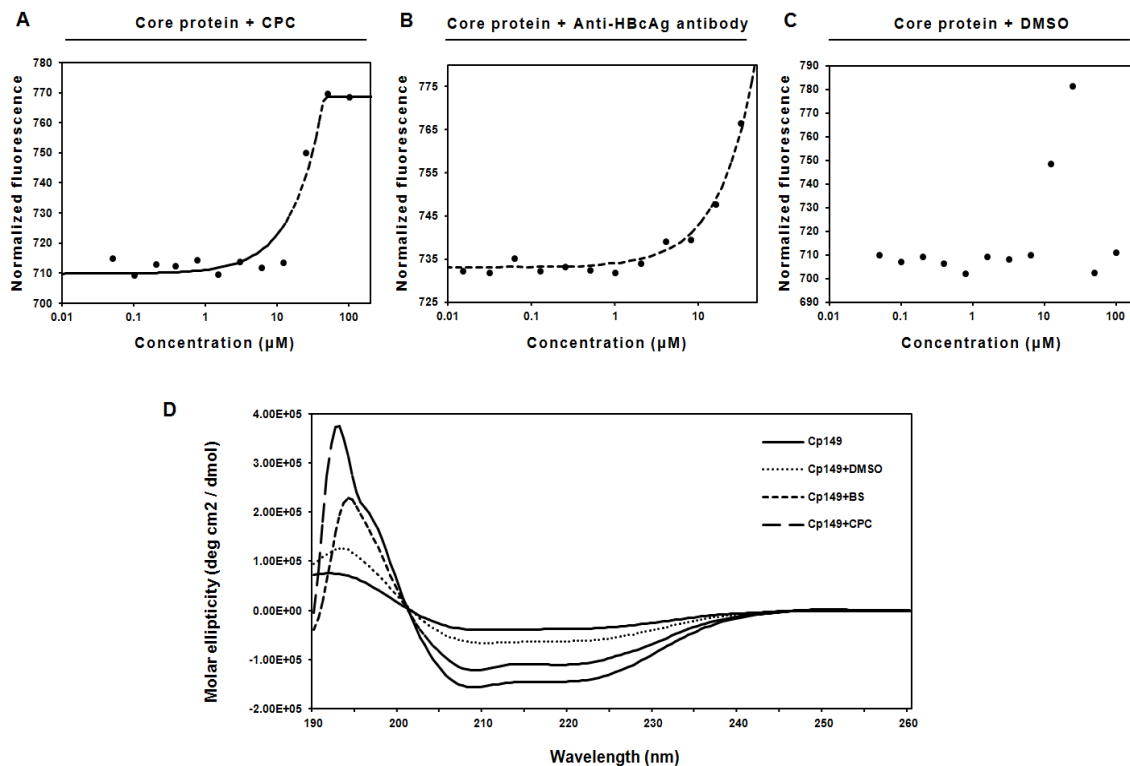


Figure 4. Interaction and conformational change of HBV Cp149 with the novel capsid assembly inhibitor CPC.

A-C. Microscale thermophoresis changes between purified Cp149 and CPC (A), Anti-HBcAg antibody (B, Positive control), and DMSO (C, Negative control). Experiments were repeated in 20, 40, 60, and 80% MST power sequences and results from 40% MST are presented in the figure. D. Molar ellipticity change in Cp149 with 1% DMSO (Negative control), 50 μM BS (Positive control), and 5 μM CPC treatment. HBV, Hepatitis B virus; Cp149, Core protein 149; DMSO, Dimethyl sulfoxide; Anti-HBcAg, Anti-Hepatitis B core antigen; BS, Benzenesulfonamide; CPC, Cetylpyridinium chloride.

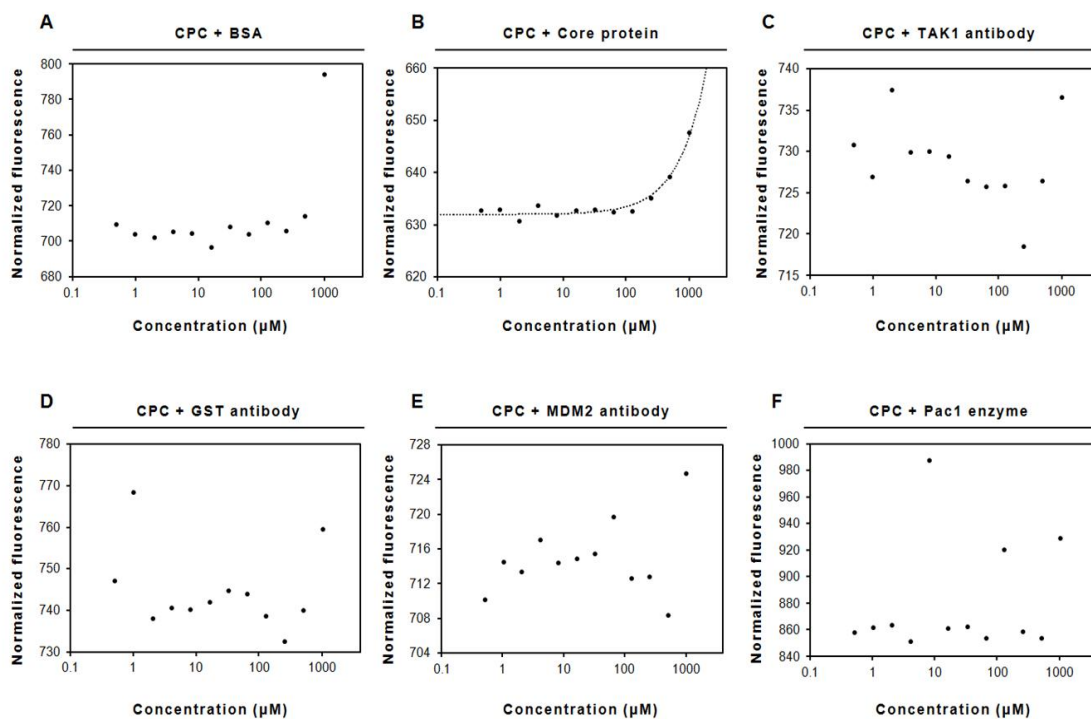


Figure 5. Interaction of CPC with diverse proteins.

A-F. Microscale thermophoresis changes between CPC and various proteins (BSA, Cp149, TAK1, GST, MDM2, Pac1). CPC, Cetylpyridinium chloride; BSA, Bovine serum albumin; TAK1, Transforming growth factor beta-activated kinase 1; GST, Glutathione S-transferase; MDM2, Mouse double minute 2 homolog.

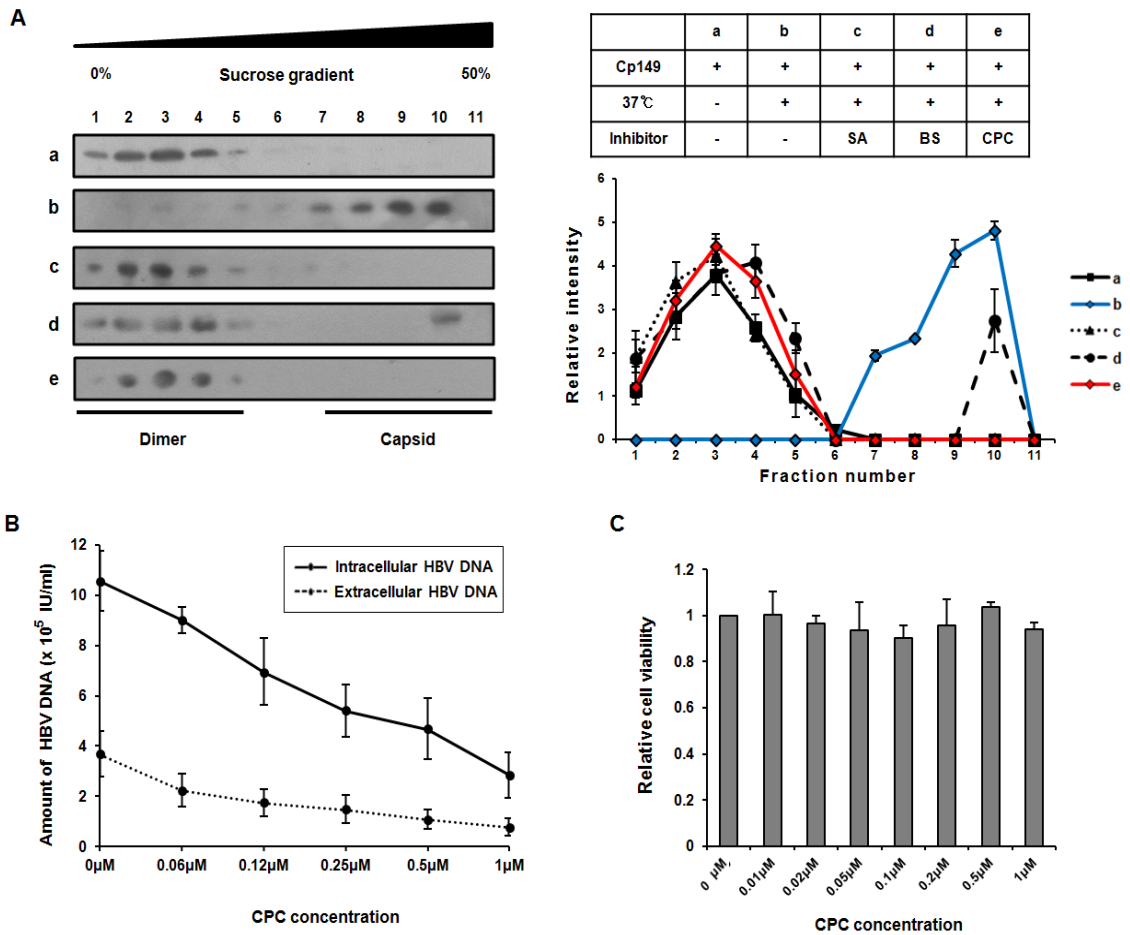


Figure 6. Inhibition of HBV capsid assembly by CPC *in vivo*.

A. Sucrose density analysis of capsid assembly with DMSO, 200 μM SA, 200 μM BS, or 20 μM CPC. B. Quantitation of HBV DNA following treatment with CPC (0-1 μM) in HepG2.2.15 cells. C. HepG2.2.15 cell viability at series of CPC concentrations. HBV, Hepatitis B virus; CPC, Cetylpyridinium chloride; DMSO, Dimethyl sulfoxide; SA, Sulfanilamide; BS, Benzenesulfonamide.

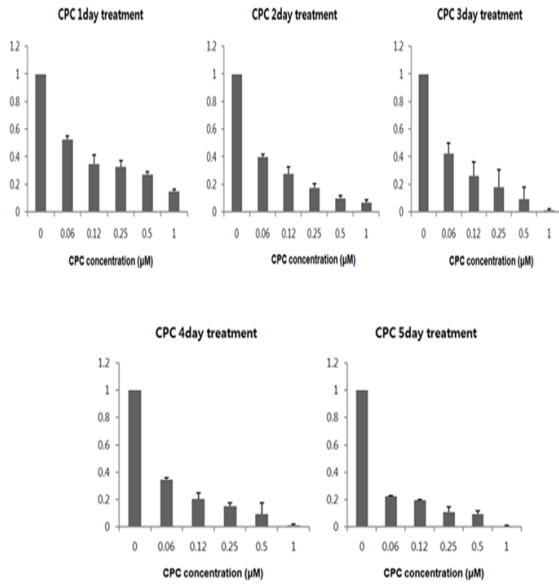
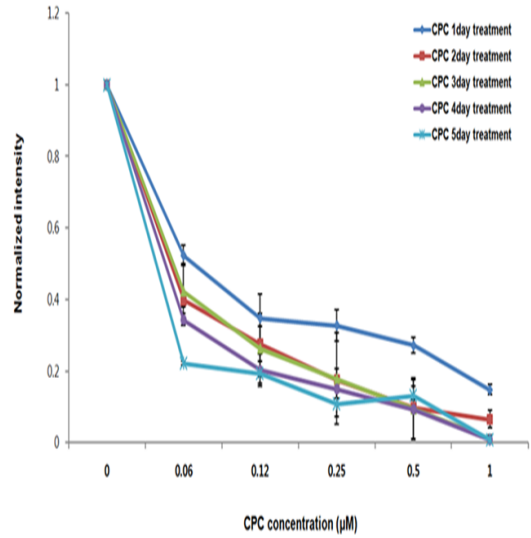
A**B**

Figure 7. Relative HBV DNA change by CPC daily treatment duration and concentration.

A. Graph of relative HBV DNA in CPC treatment concentrations (0/0.06/0.12/0.25/0.5/1 μM) for different CPC daily (0/1/2/3/4/5 day) treatment durations. B. Graph of relative HBV DNA change by CPC daily treatment duration and concentration.

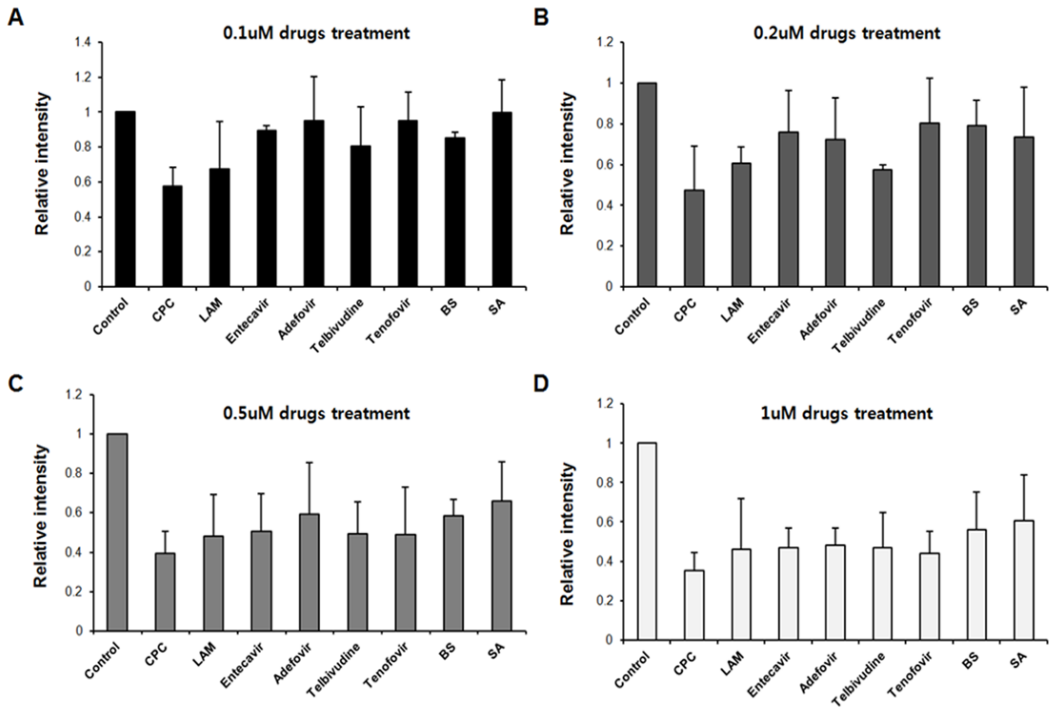


Figure 8. Comparison of HBV DNA inhibition between CPC and other nucleos(t)ide analogues. A-D. Relative HBV DNA change after treatment of CPC and nucleos(t)ide analogues at (0.1/0.2/0.5/1μM) concentration, 24h. CPC, Cetylpyridinium chloride; LAM, Lamivudine; BS, Benzenesulfonamide; SA, Sulfanilamide.

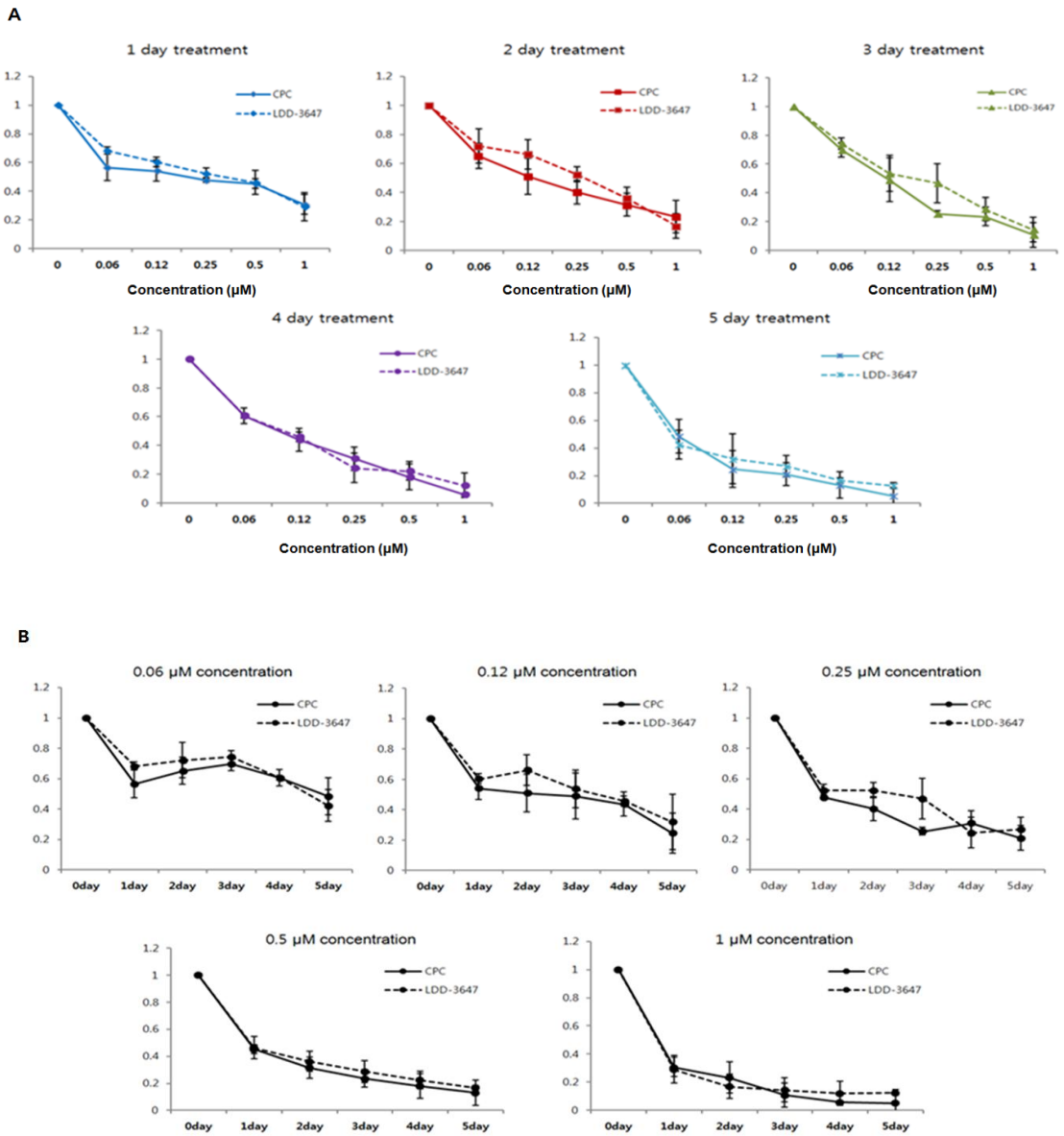


Figure 9. Comparison of CPC and LDD-3647 as HBV DNA inhibitors.

A. Relative HBV DNA change between CPC and LDD-3647 by treatment concentration

(0/0.06/0.12/0.25/0.5/1 μM) in different treatment durations (0/1/2/3/4/5 day). B. Relative HBV

DNA change between CPC and LDD-3647 by treatment duration (0/1/2/3/4/5 day) in different

treatment concentrations (0/0.06/0.12/0.25/0.5/1 μM).

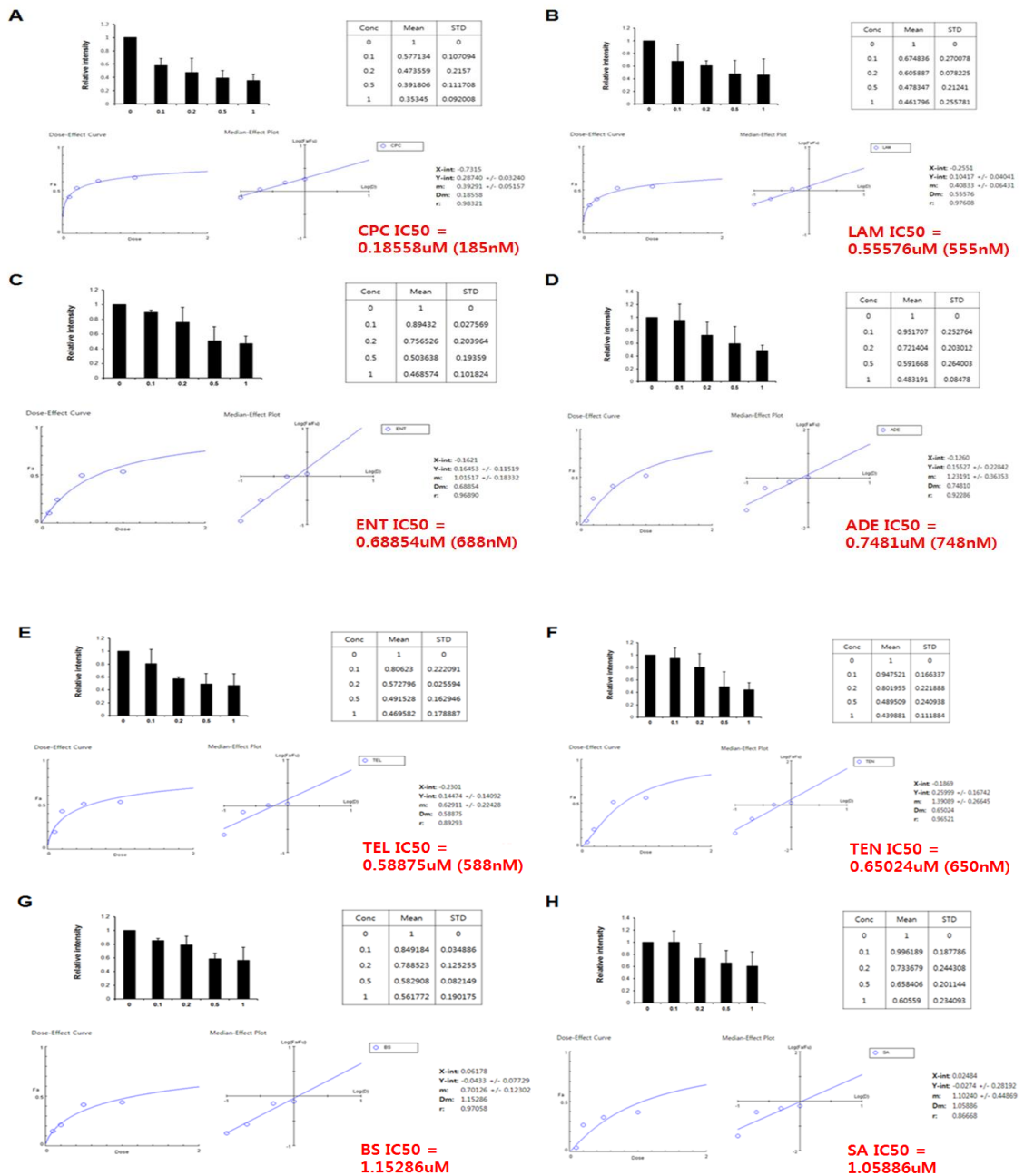


Figure 10. IC50 values and HBV DNA change for HBV capsid inhibitor and nucleos(t)ide analogues.

A-H. IC50 value and relative HBV DNA change by various drugs (CPC, LAM, ENT, ADE, TEL, TEN, BS, SA) treatment concentrations (0/0.06/0.12/0.25/0.5/1µM).

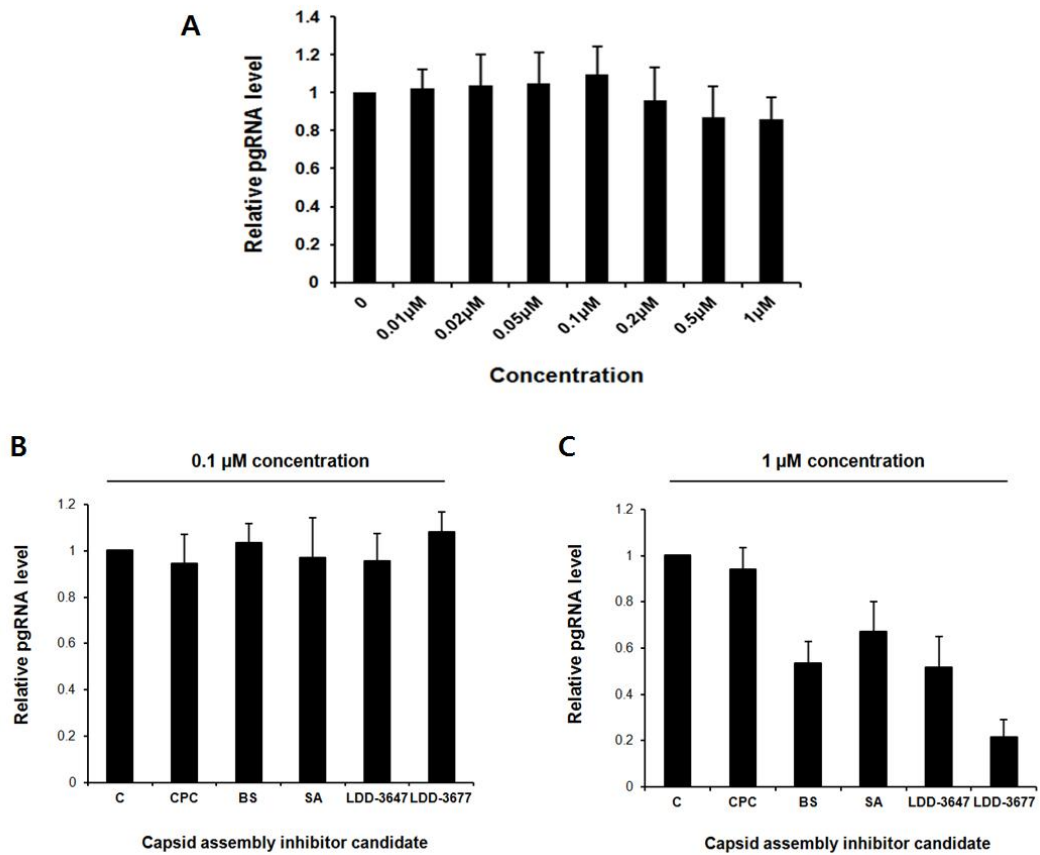


Figure 11. Relative pgRNA levels after various drugs treatments in HepG2.2.15 cell.

A. Relative DNA quantity at the pgRNA transcription step of the HBV life cycle from HepG2.2.15 in a series of varying CPC concentration treatment. B. Relative pgRNA levels after low concentration (0.1 μM) treatment of capsid assembly inhibitors. C. Relative pgRNA levels after high concentration (1 μM) treatment of capsid assembly inhibitors. HBV, Hepatitis B virus; CPC, Cetylpyridinium chloride; BS, Benzenesulfonamide; SA, Sulfanilamide.

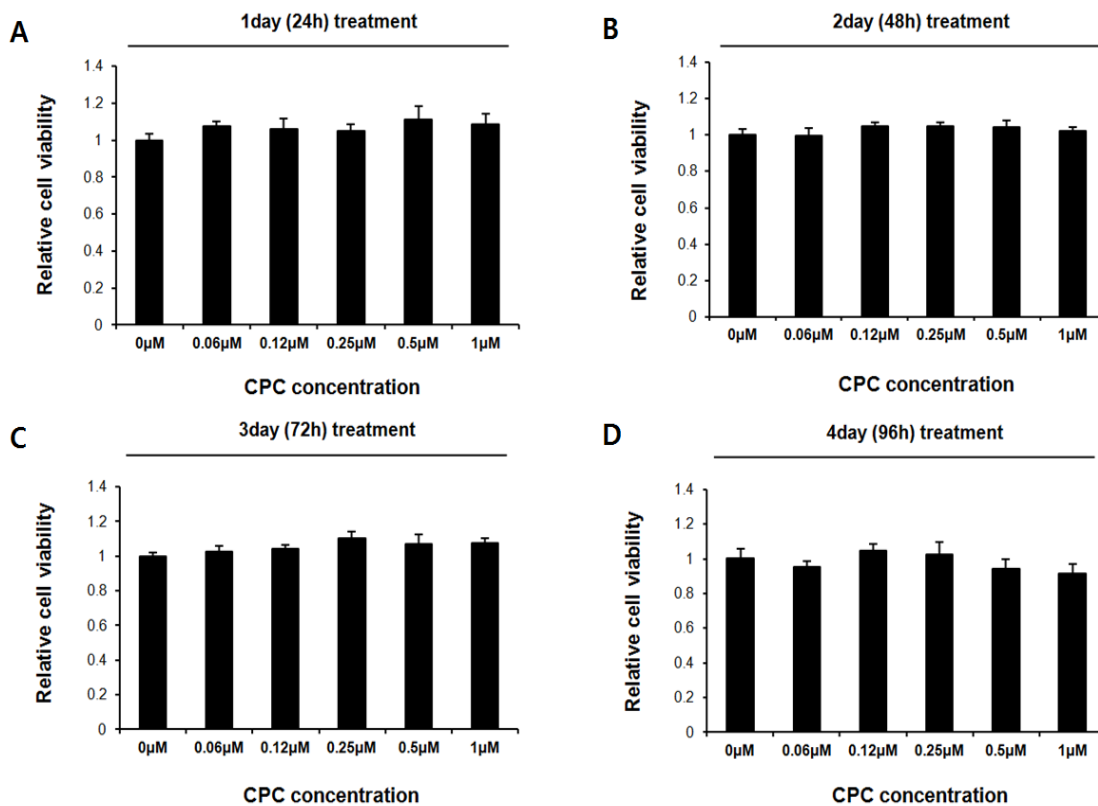


Figure 12. HepG2.2.15 cell viability in CPC daily treatment in different durations and concentrations.

A-D. Relative cell viability for 1day (24/48/72/96h) CPC concentration with different concentrations. HBV, Hepatitis B virus; CPC, Cetylpyridinium chloride; DMSO, Dimethyl sulfoxide; SA, Sulfanilamide; BS, Benzenesulfonamide.

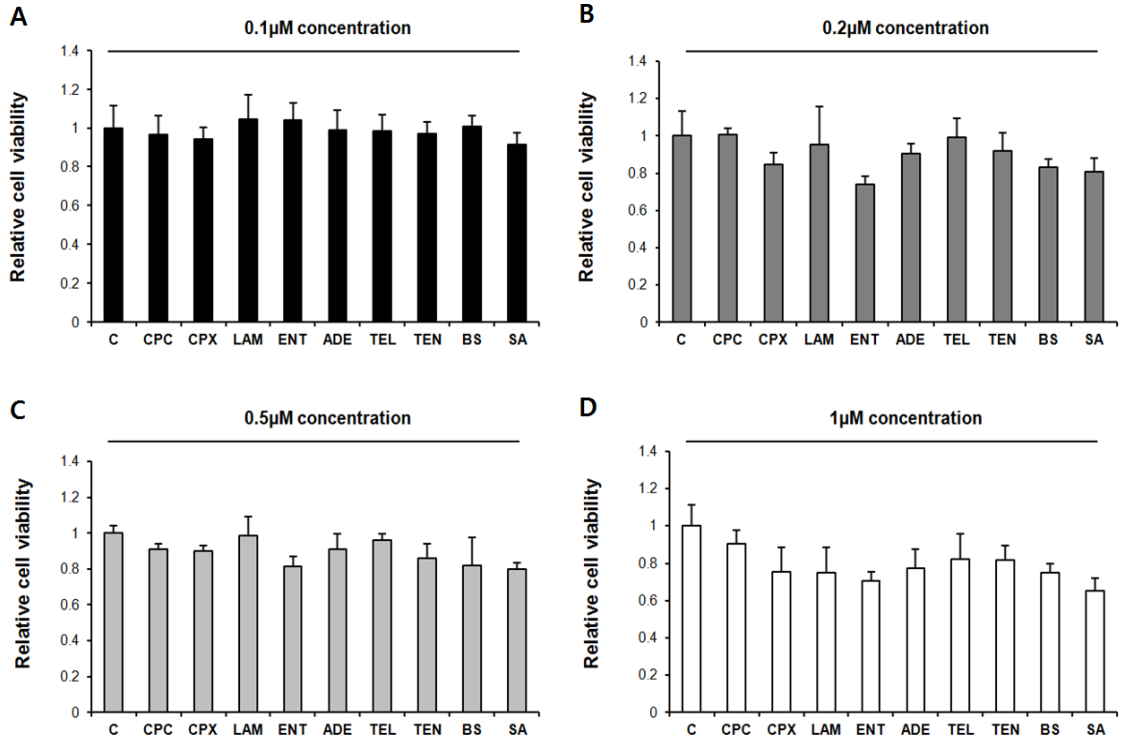


Figure 13. Comparison of drug cytotoxicity after drug treatments in HepG2.2.15.

A-D. Relative cell viability after drug treatments in (0.1/0.2/0.5/1 μM) concentration. CPC, Cetylpyridinium chloride; CPX, Ciclopirox; LAM, Lamivudine; ENT, Entecavir; ADE, Adefovir; TEL, Telbivudine; TEN, Tenofovir; BS, Benzenesulfonamide; SA, Sulfanilamide.

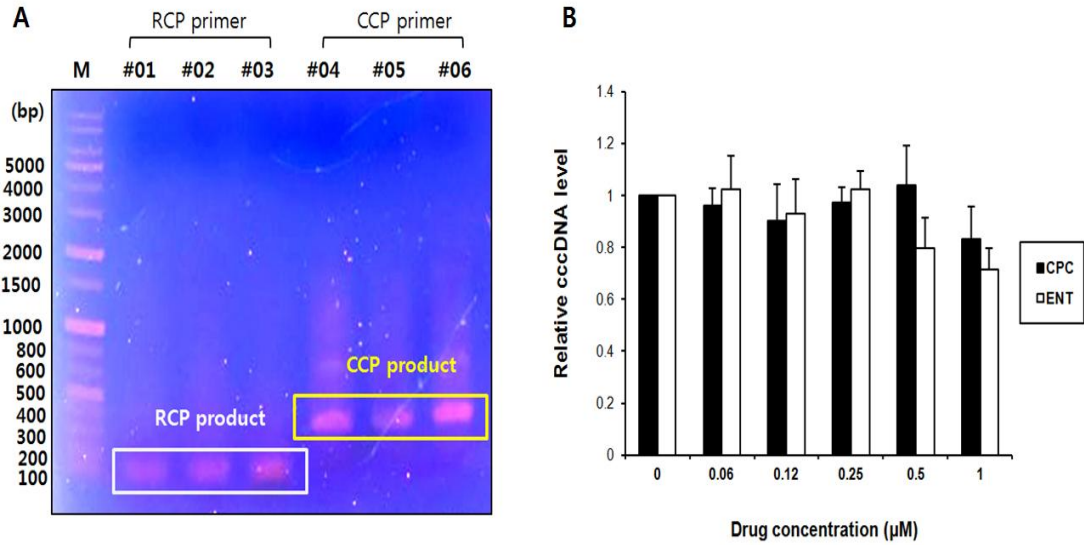


Figure 14. Comparison of HBV cccDNA level change by treatment concentration between CPC and ENT.

A. Confirmation of extracted HBV cccDNA using PCR. Only cccDNA contains both RCP and CCP regions. B. Relative change in HBV cccDNA levels after different CPC and ENT concentration treatments. HBV, Hepatitis B virus ; cccDNA. covalently closed circular DNA; CPC, Cetylpyridinium chloride; ENT, Entecavir.

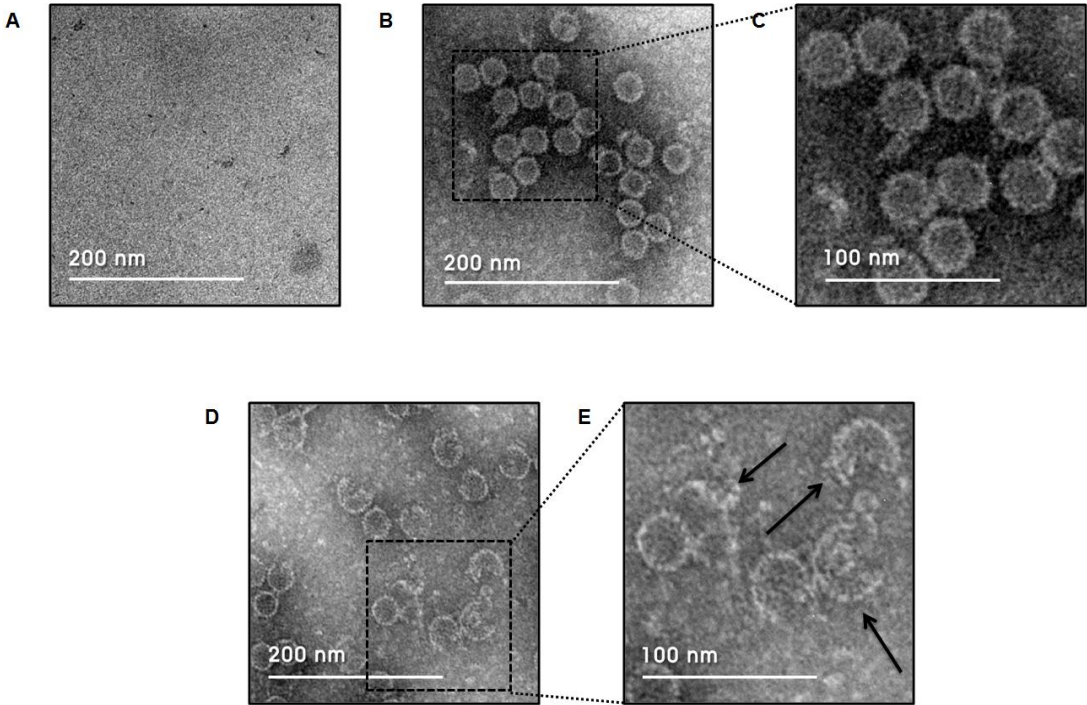


Figure 15. Transmission electron micrographs of untreated and CPC-treated Cp149 capsids.

A. Non-assembled Cp149. B. Fully assembled Cp149 in reaction buffer at 37°C with no treatment.

C. Magnified image of fully assembled capsid particle with no treatment. D. Assembled Cp149

with 20 μM CPC treatment. E. Magnified image of broken capsid particles after 20 μM CPC treatment. Cp149, Core protein 149; CPC, Cetylpyridinium chloride.

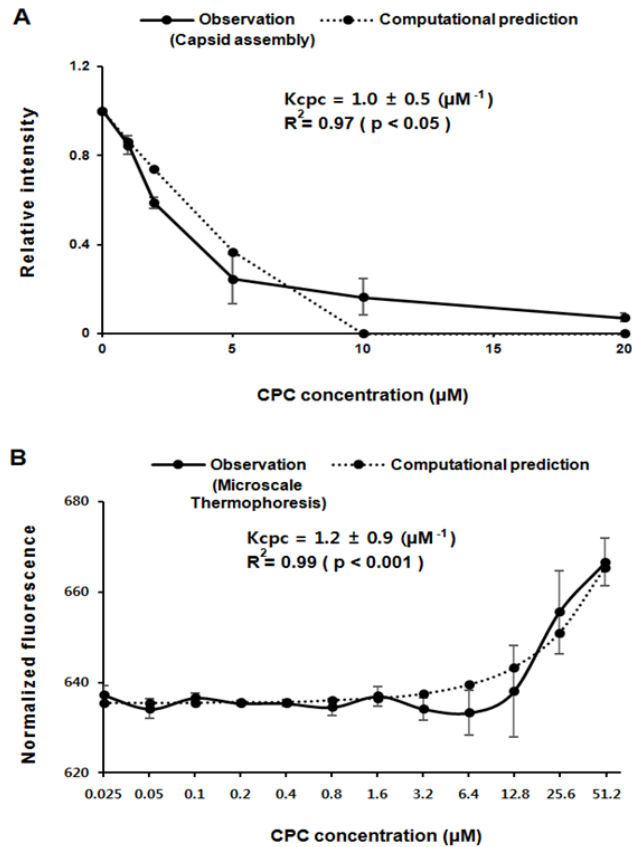


Figure 16. Numerical interpretation of capsid assembly inhibition.

A. Capsid assembly assay with HBV Cp149 in a series of CPC concentrations. Relative capsid amount was quantified from the intensity of bands obtained by immunoblot analysis. Assembly inhibition curve and computationally extrapolated prediction curve were plotted. B. Microscale thermophoresis assay with HBV Cp149 in a series of CPC concentrations. Normalized fluorescence intensity was interpreted by the superpositional expression of thermophoresis between capsid and dimer. Thermophoresis curve and computationally derived prediction curve were plotted. CPC association constant, R square and P-value were noted.

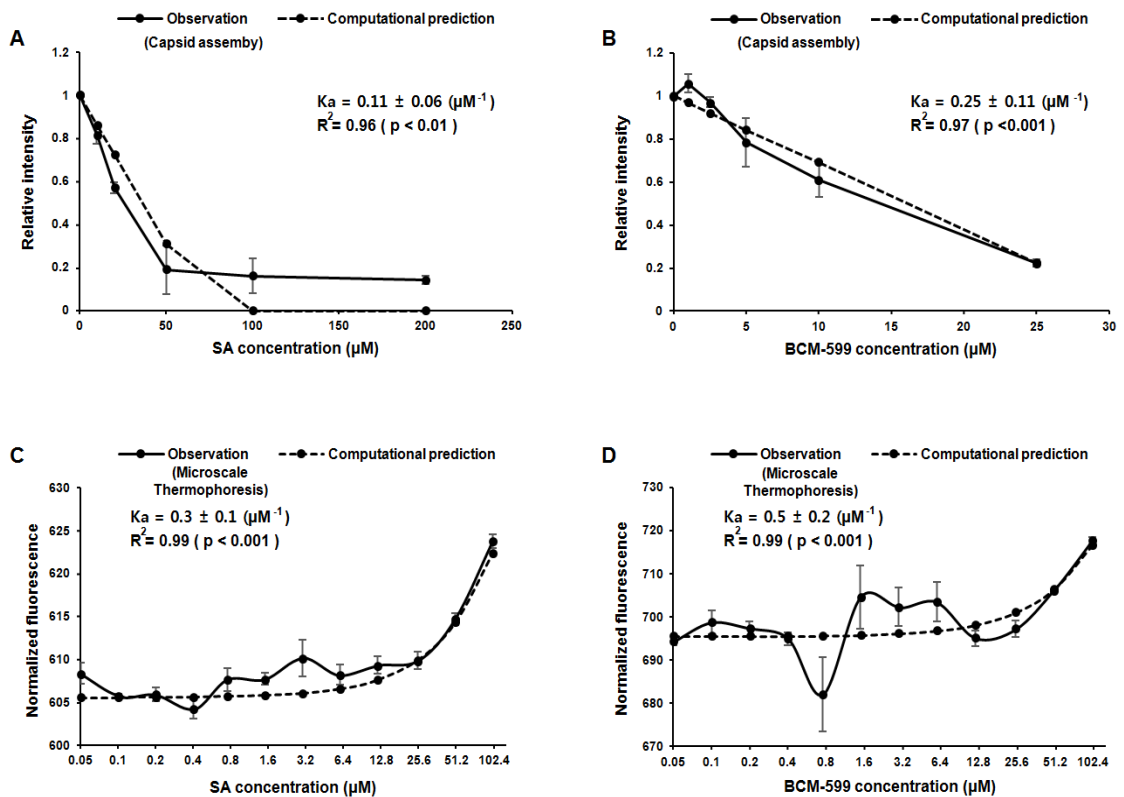


Figure 17. Numerical interpretation of capsid assembly inhibition for SA and BCM-599.

A-B. Capsid assembly assay with HBV Cp149 at a series of SA (A) and BCM-599 (B) concentrations. Assembly inhibition curve and computationally extrapolated prediction curve were plotted. Association constant (K_a), R square, and P-value were noted. C-D. Microscale thermophoresis assay with HBV Cp149 at series of SA (C) and BCM-599 (D) concentrations. Thermophoresis curve and computationally derived prediction curve were plotted. Association constant (K_a), R square and P-value were noted.

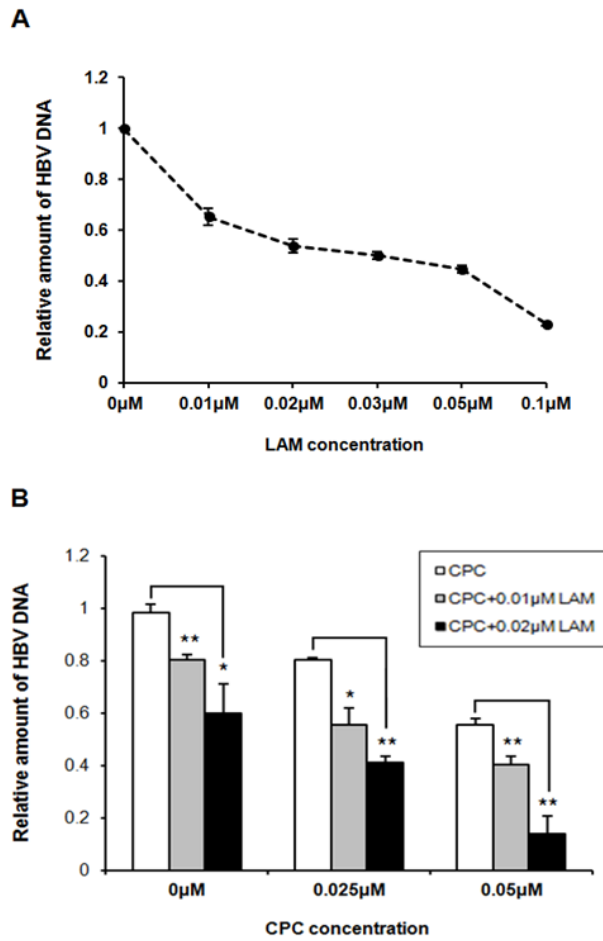


Figure 18. Antiviral activity of combinational effect between CPC and LAM.

A. Virion concentrations after LAM gradient treatment (0-0.1 μM). B. Relative virion concentrations after different combination treatments with CPC and LAM. CPC, Cetylpyridinium chloride; LAM, Lamivudine; HBV, Hepatitis B virus.

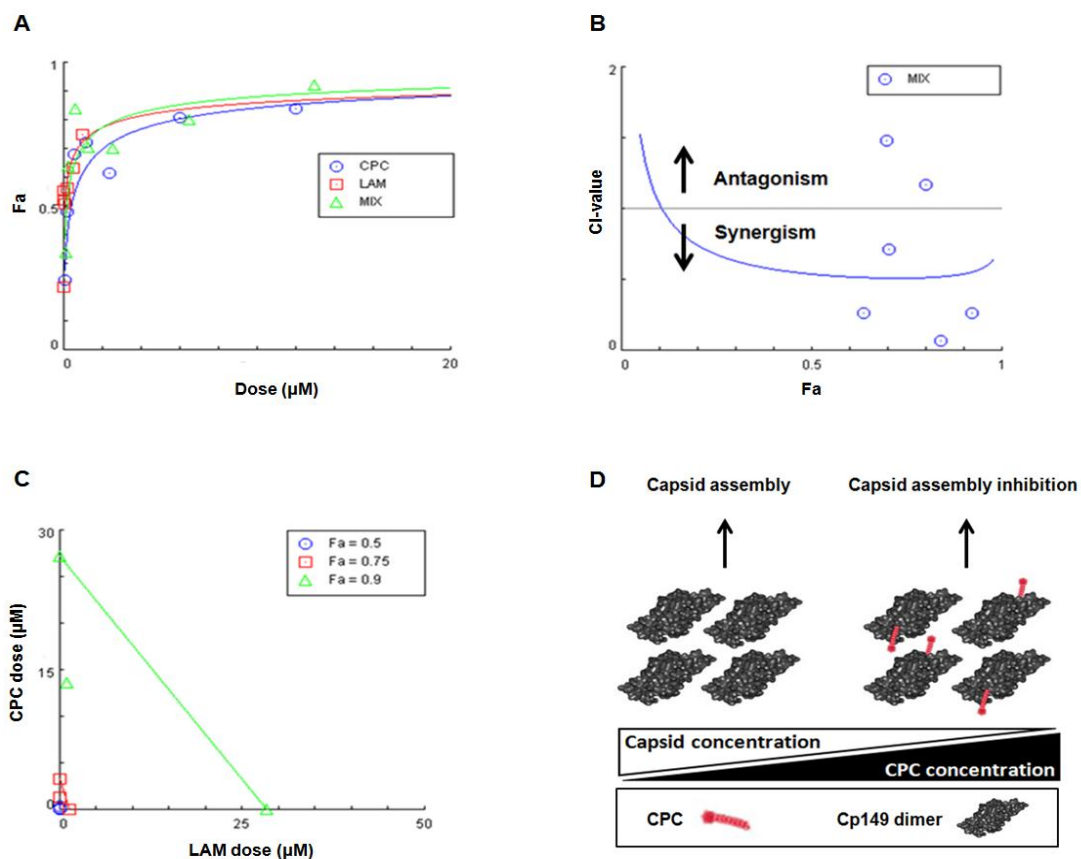


Figure 19. The graphical representations obtained from the CompuSyn Report and schematic of capsid assembly inhibition.

A. Dose-effect curve. Fractional effect value (Fa) on the y-axis indicates fraction of reduced HBV virion. B. Combination index plot. Concentration ratio of CPC to LAM was fixed to 12. CI values at CPC and LAM concentrations corresponding to given fractional effect value were plotted. C. Isobologram with CPC to LAM concentration ratio at 12. Additive lines in given fractional effect values indicate CPC and LAM concentrations that result in additive effect between two compounds. D. Cp149 dimer is depicted in monochrome, solid rendered surface and CPC are highlighted in red. CPC is bound to Cp149 dimer. Capsid formation is inversely correlated with CPC concentration.

Table 1. ADMET property of HBV inhibitor candidates.

Name	FDA approved drug number	ADMET									
		Solubility	PPB level	Hepatotoxicity probability	CYP2D6 probability	AlogP98	PSA 2D	Absorption-95	Absorption-99	BBB-95	BBB-99
Sulfanilamide (SA)		-0.891	0	0.649	0.039	-0.212	87.681	✓	✓	✓	✓
Benzenesulfonamide (BS)		-1.365	0	0.536	0.049	0.535	61.141	✓	✓		✓
Idoxuridine (IDO)	357	-0.213	0	0.761	0.099	-1.208	101.325		✓		
Cetylpyridinium chloride (CPC)	849	-6.305	2	0.589	0.722	7.584	5.348				
Amoxicillin (AMO)	649	-2.523	0	0.364	0.445	-0.06	136.236		✓		
Tripelennamine HCl (TPH)	704	-3.702	1	0.635	0.881	3.102	17.965	✓	✓	✓	✓
Fluocinonide (FLU)	632	-3.88	0	0.344	0.326	1.374	99.508	✓	✓		✓
Gliquidone (GLI)	708	-5.735	2	0.344	0.297	4.738	124.406				
Rofecoxib (RFC)	666	-4.258	1	0.701	0.514	2.871	60.832	✓	✓	✓	✓
Amlodipine besylate (AML)	326	-3.593	2	0.284	0.495	1.576	100.742	✓	✓		✓
Clozapine (CLZ)	534	-5.176	2	0.238	0.732	3.476	30.838	✓	✓	✓	✓
Tetracycline HCl (TET)	610	-2.648	0	0.854	0.326	-1.011	185.872				
Entecavir		-0.528	0	0.39	0.396	-1.404	126.214		✓		
Tenofovir		-1.086	0	0.748	0.148	-0.911	133.533		✓		
Adefovir		-3.546	0	0.331	0.326	1.899	162.224				
Lamivudine		-0.83	0	0.364	0.059	-0.59	88.262	✓	✓		✓
Telbivudine		-0.102	0	0.801	0.039	-1.044	101.325	✓	✓		

ADMET analysis was conducted based on six distinct criteria. Solubility in log S value was predicted as an important determinant in absorption. Plasma protein binding (PPB) affinity level and blood brain barrier (BBB) penetration confidence status were introduced as distribution criteria. Cytochrome P450 2D6 (CYP2D6), an enzyme deeply involved in xenobiotic metabolism, was subjected to inhibition probability computation for drug metabolism and excretion evaluation. Hepatotoxicity probability was predicted among other toxicities. Molecular partition coefficient (AlogP98) and polar surface area (PSA2D) values were plotted showing absorption and blood.

Table 2. Capsid particle classification.

Number	Capsid counts			Total counts
	Normal	Broken	Abnormal forms	
Non-assembled	40	2 (4.65%)	1 (2.32%)	43
Fully assembled	944	49 (4.78%)	31 (3.02%)	1024
Cetylpyridinium chloride	83	203 (51.26%)	110 (27.77%)	396

Capsid particles in each case, pre-reaction, post-reaction, and post-reaction with 20 μ M CPC treatment, were counted and classified into one of the following categories: normal capsid, broken capsid, and abnormal capsid. Broken capsid was defined as those that resemble normal capsids, but with significantly disrupted spherical structures. Abnormal capsids have significant size but, resemble neither normal capsid nor broken capsid. Most particles classified as abnormal capsids were amorphous aggregates with similar sizes as capsids.

Table 3. Inhibitor affinity derived in numerical interpretation.

Name	Capsid assembly		Microscale thermophoresis	
	association constant	R square	association constant	R square
Cetylpyridinium Chloride(CPC)	1.0±0.5 (uM ⁻¹)	0.97	1.2±0.9 (uM ⁻¹)	0.99
Sulfanilamide(SA)	0.11±0.06 (uM ⁻¹)	0.96	0.3±0.1 (uM ⁻¹)	0.99
BCM-599	0.25±0.11 (uM ⁻¹)	0.99	0.5±0.2 (uM ⁻¹)	0.99

Capsid assembly and microscale thermophoresis results were interpreted based on the non-competitive inhibition model. Inhibitor association constants for CPC, SA, and BCM-599 were derived from arithmetic operations. R square values for the fit curve were marked separately.

Table 4. IC₅₀ values and CI index of inhibitor CPC-LAM cocktails.

Combination ratio	IC ₅₀ (μ M)	CI-value	Synergic effect
Pure CPC	0.25	1	
12 : 1	0.154	0.551	+++
4 : 1	0.140	0.376	+++
3 : 1	0.145	0.796	++
2 : 1	0.102	0.803	++
1.5 : 1	0.105	0.811	++
1 : 1	0.079	0.875	+
0.67 : 1	0.076	0.862	+
0.5 : 1	0.078	1.110	-
0.33 : 1	0.065	0.920	\pm
Pure 3TC	0.023	1	

Variable combinational treatment of CPC and LAM was analyzed using the compusyn program. Combination ratio defined as CPC concentration to LAM concentration (12, 4, 3, 2, 1.5, 1, 0.67, 0.5, and 0.33: 1) were treated with LAM concentrations (0.01, 0.02, 0.05, 0.1, 0.2, 0.5, and 1 μ M). HepG2.2.15 extracellular HBV DNA was collected and quantified using real time PCR. Drug inhibitory effect was calculated as the fraction of decrease in HBV viral DNA compared to the control. IC₅₀ (μ M) and CI-values were analyzed for individual ratios. Synergistic effect is marked from normal indication for reference.

Table 5. Equations used in numerical analysis of capsid assembly inhibition.

Equation number	Formula	Description
Eq. 1.	$Cp149_2 + CPC \rightleftharpoons Cp149_2 \cdot CPC$	CPC binding equilibrium
Eq. 2.	$120Cp149_2 \rightleftharpoons Capsid$	Capsid assembly equilibrium
Eq. 3.	$[Cp149_2]_{Total} = 120[Capsid] + [Cp149_2] + [Cp149_2 \cdot CPC]$	Core protein conservation
Eq. 4.	$[CPC]_{Total} = [Cp149_2 \cdot CPC] + [CPC]$	CPC conservation
Eq. 5.	$K_{capsid} = [Capsid]/[Cp149_2]^{120}$	Core association constant
Eq. 6.	$[Cp149_2]_{Total} = 120[Capsid] + \sqrt[120]{[Capsid]/K_{capsid}} + [Cp149_2 \cdot CPC]$	Core protein conservation recasted
Eq. 7.	$K_{CPC} = \frac{[Cp149_2 \cdot CPC]}{([CPC]_{Total} - [Cp149_2 \cdot CPC]) \sqrt[120]{[Capsid]/K_{capsid}}}$	CPC association constant
Eq. 8.	$F_{norm} = \frac{25[Capsid](1 - 50S_T\Delta T) + ([Cp149_2] + [Cp149_2 \cdot CPC])(1 - S_T\Delta T)}{25[Capsid] + [Cp149_2] + [Cp149_2 \cdot CPC]}$	Thermophoresis fluorescence intensity

Equilibrium of CPC binding reaction (Eq. 1.) and capsid assembly reaction (Eq. 2.) were set as a competing equilibrium by sharing dimeric core protein term in both equations. Mass conservation law for core protein conservation (Eq. 3.) and CPC conservation (Eq. 4.) were formulated with concentration terms. Core association constant was derived from capsid assembly reaction equilibrium (Eq. 5.). Core protein conservation equation was recasted in terms of capsid and CPC bound dimeric core protein concentration terms using core protein association constant (Eq. 6.). CPC association constant was derived from CPC binding reaction equilibrium (Eq. 7.). CPC association constant equation was used to obtain CPC association constants. Normalized fluorescence intensity in core protein thermophoresis was formulated as a superposition of normalized fluorescence intensity terms of capsid, CPC bound core protein dimer, and unbound core protein dimer (Eq. 8.)

Reference

- Baaske, P., Wienken, C.J., Reineck, P., Duhr, S., Braun, D., 2010. Optical thermophoresis for quantifying the buffer dependence of aptamer binding. *Angew Chem Int Ed Engl* 49, 2238-2241.
- Brunetto, M.R., Lok, A.S., 2010. New approaches to optimize treatment responses in chronic hepatitis B. *Antivir Ther* 15 Suppl 3, 61-68.
- Cho, M.H., Jeong, H., Kim, Y.S., Kim, J.W., Jung, G., 2014. 2-amino-N-(2,6-dichloropyridin-3-yl)acetamide derivatives as a novel class of HBV capsid assembly inhibitor. *J Viral Hepat* 21, 843-852.
- Cho, M.H., Song, J.S., Kim, H.J., Park, S.G., Jung, G., 2013. Structure-based design and biochemical evaluation of sulfanilamide derivatives as hepatitis B virus capsid assembly inhibitors. *J Enzyme Inhib Med Chem* 28, 916-925.
- Chou, T.C., 2006. Theoretical basis, experimental design, and computerized simulation of synergism and antagonism in drug combination studies. *Pharmacol Rev* 58, 621-681.
- Chou, T.C., 2010. Drug Combination Studies and Their Synergy Quantification Using the Chou-Talalay Method. *Cancer Res* 70, 440-446.
- Dawood, A., Abdul Basit, S., Jayaraj, M., Gish, R.G., 2017. Drugs in Development for Hepatitis B. *Drugs* 77, 1263-1280.
- Doong, S.L., Tsai, C.H., Schinazi, R.F., Liotta, D.C., Cheng, Y.C., 1991. Inhibition of the replication of hepatitis B virus in vitro by 2',3'-dideoxy-3'-thiacytidine and related analogues. *Proc Natl Acad Sci U S A* 88, 8495-8499.
- Fabrizi, F., Dulai, G., Dixit, V., Bunnapradist, S., Martin, P., 2004. Lamivudine for the treatment of hepatitis B virus-related liver disease after renal transplantation: meta-analysis of clinical trials. *Transplantation* 77, 859-864.

Garson, J.A., Grant, P.R., Ayliffe, U., Ferns, R.B., Tedder, R.S., 2005. Real-time PCR quantitation of hepatitis B virus DNA using automated sample preparation and murine cytomegalovirus internal control. *J Virol Methods* 126, 207-213.

Hirsch, R.C., Lavine, J.E., Chang, L.J., Varmus, H.E., Ganem, D., 1990. Polymerase gene products of hepatitis B viruses are required for genomic RNA packaging as well as for reverse transcription. *Nature* 344, 552-555.

Kang, H.Y., Lee, S., Park, S.G., Yu, J., Kim, Y., Jung, G., 2006. Phosphorylation of hepatitis B virus Cp at Ser87 facilitates core assembly. *Biochem J* 398, 311-317.

Kim, Y.S., Seo, H.W., Jung, G., 2015. Reactive oxygen species promote heat shock protein 90-mediated HBV capsid assembly. *Biochem Biophys Res Commun* 457, 328-333.

Lee, J.E., Lee, J.M., Lee, Y., Park, J.W., Suh, J.Y., Um, H.S., Kim, Y.G., 2017. The antiplaque and bleeding control effects of a cetylpyridinium chloride and tranexamic acid mouth rinse in patients with gingivitis. *J Periodontal Implant Sci* 47, 134-142.

Lee, M.J., Song, H.J., Jeong, J.Y., Park, S.Y., Sohn, U.D., 2013. Anti-Oxidative and Anti-Inflammatory Effects of QGC in Cultured Feline Esophageal Epithelial Cells. *Korean J Physiol Pharmacol* 17, 81-87.

Leis, S., Schneider, S., Zacharias, M., 2010. In silico prediction of binding sites on proteins. *Curr Med Chem* 17, 1550-1562.

Lott, L., Beames, B., Notvall, L., Lanford, R.E., 2000. Interaction between hepatitis B virus core protein and reverse transcriptase. *J Virol* 74, 11479-11489.

Meleshyn, A., 2009. Cetylpyridinium chloride at the mica-water interface: incomplete monolayer and bilayer structures. *Langmuir* 25, 881-890.

- Ott, J.J., Stevens, G.A., Groeger, J., Wiersma, S.T., 2012. Global epidemiology of hepatitis B virus infection: new estimates of age-specific HBsAg seroprevalence and endemicity. *Vaccine* 30, 2212-2219.
- Pan, H.Y., Pan, H.Y., Song, W.Y., Zheng, W., Tong, Y.X., Yang, D.H., Dai, Y.N., Chen, M.J., Wang, M.S., Huang, Y.C., Zhang, J.J., Huang, H.J., 2017. Long-term outcome of telbivudine versus entecavir in treating higher viral load chronic hepatitis B patients without cirrhosis. *J Viral Hepat* 24 Suppl 1, 29-35.
- Paradis, V., 2013. Histopathology of hepatocellular carcinoma. *Recent Results Cancer Res* 190, 21-32.
- Popkin, D.L., Zilka, S., Dimaano, M., Fujioka, H., Rackley, C., Salata, R., Griffith, A., Mukherjee, P.K., Ghannoum, M.A., Esper, F., 2017. Cetylpyridinium Chloride (CPC) Exhibits Potent, Rapid Activity Against Influenza Viruses in vitro and in vivo. *Pathog Immun* 2, 252-269.
- Rao, S.N., Head, M.S., Kulkarni, A., LaLonde, J.M., 2007. Validation studies of the site-directed docking program LibDock. *J Chem Inf Model* 47, 2159-2171.
- Ren, Q., Liu, X., Luo, Z., Li, J., Wang, C., Goldmann, S., Zhang, J., Zhang, Y., 2017. Discovery of hepatitis B virus capsid assembly inhibitors leading to a heteroaryldihydropyrimidine based clinical candidate (GLS4). *Bioorg Med Chem* 25, 1042-1056.
- Seeger, C., Mason, W.S., 2000. Hepatitis B virus biology. *Microbiol Mol Biol Rev* 64, 51-68.
- Shim, H.Y., Quan, X., Yi, Y.S., Jung, G., 2011. Heat shock protein 90 facilitates formation of the HBV capsid via interacting with the HBV core protein dimers. *Virology* 410, 161-169.
- Smith, J.R., Evans, K.J., Wright, A., Willows, R.D., Jamie, J.F., Griffith, R., 2012. Novel indoleamine 2,3-dioxygenase-1 inhibitors from a multistep in silico screen. *Bioorg Med Chem* 20, 1354-1363.

Stein, L.L., Loomba, R., 2009. Drug targets in hepatitis B virus infection. *Infect Disord Drug Targets* 9, 105-116.

Timofeeva, O.A., Chasovskikh, S., Lonskaya, I., Tarasova, N.I., Khavrutskii, L., Tarasov, S.G., Zhang, X., Korostyshevskiy, V.R., Cheema, A., Zhang, L., Dakshanamurthy, S., Brown, M.L., Dritschilo, A., 2012. Mechanisms of unphosphorylated STAT3 transcription factor binding to DNA. *J Biol Chem* 287, 14192-14200.

Vanlandschoot, P., Cao, T., Leroux-Roels, G., 2003. The nucleocapsid of the hepatitis B virus: a remarkable immunogenic structure. *Antiviral Res* 60, 67-74.

Venkatachalam, C.M., Jiang, X., Oldfield, T., Waldman, M., 2003. LigandFit: a novel method for the shape-directed rapid docking of ligands to protein active sites. *J Mol Graph Model* 21, 289-307.

Wu, G., Robertson, D.H., Brooks, C.L., 3rd, Vieth, M., 2003. Detailed analysis of grid-based molecular docking: A case study of CDOCKER-A CHARMM-based MD docking algorithm. *J Comput Chem* 24, 1549-1562.

Wynne, S.A., Crowther, R.A., Leslie, A.G., 1999. The crystal structure of the human hepatitis B virus capsid. *Mol Cell* 3, 771-780.

Yang, L., Lu, M., 2017. Small molecule inhibitors of hepatitis B virus nucleocapsid assembly: a new approach to treat chronic HBV infection. *Curr Med Chem*.

Zlotnick, A., Ceres, P., Singh, S., Johnson, J.M., 2002. A small molecule inhibits and misdirects assembly of hepatitis B virus capsids. *J Virol* 76, 4848-4854.

Zuckerman, A.J., 1999. More than third of world's population has been infected with hepatitis B virus. *BMJ* 318, 1213.

Chapter 3

**Heat shock protein 70 and Heat shock protein 90
synergistically increase hepatitis B viral capsid assembly**

Introduction

The hepatitis B virus (HBV), belonging to the family of Hepadnaviridae, is a pathogen that causes acute and chronic hepatitis (Chisari and Ferrari, 1995; Gust et al., 1986). More than three billion people worldwide are infected with HBV (Zuckerman, 1999a). Around 240 million people suffer from chronic conditions, associated with the development of liver cirrhosis and hepatocellular carcinoma (HCC) (Ott et al., 2012).

HBV contains a partially double-stranded DNA genome with four overlapping open reading frames (ORFs) that encodes core protein, surface protein, polymerase, and X protein. In the viral life cycle, the HBV genome is converted into covalently closed circular DNA and transcribed into pregenomic RNA (pgRNA) (Seeger and Mason, 2000). An icosahedral nucleocapsid assembled from the core protein encapsidates the pgRNA polymerase (Bartenschlager and Schaller, 1992; Crowther et al., 1994). The HBV core protein comprises 183 amino acids and consists of two functional domains, the N-terminal core assembly domain (amino acids 1-149) and the C-terminal nucleic acid-binding domain (amino acids 150-183). We used core protein 149 (Cp149), C-terminal truncated, core protein assembly domain to assess effects on capsid assembly (Birnbaum and Nassal, 1990). Cp149 is capable of forming capsid-like particles *in vitro* (Gallina et al., 1989). Cp149 dimers congregate in a hexamer unit to act as a nucleus for capsid assembly stabilization (Wynne et al., 1999).

In our previous studies, nucleophosmin (B23) and heat shock protein 90 (Hsp90) were

shown to affect HBV capsid assembly *in vitro* and *in vivo* (Jeong et al., 2014; Shim et al., 2011). However, the effect of heat shock protein 70 (Hsp70) is so far unknown. Hsp70 and Hsp90 are components of a molecular chaperones network and work together as a multiprotein machinery (Pratt and Toft, 2003). They are increasingly overexpressed with the progression of HCC (Lim et al., 2005). Complexes of Hsp70 and Hsp90 including a HOP cofactor protein act as a chaperone machinery (Chen et al., 1996; Pratt and Toft, 2003). Moreover, both heat shock proteins are encapsidated in HBV particles and build polymerase-chaperone complexes that affect nucleocapsid assembly and viral DNA synthesis (Hu et al., 1997).

Based on these facts, we speculated that Hsp70 may affect HBV capsid assembly. In this study, we aimed to determine the effect of Hsp70, and synergistic effects between Hsp70 and Hsp90 affecting HBV capsid assembly. We report the effects of Hsp70 and its synergism with Hsp90 in increasing the HBV capsid assembly through interaction with core protein dimers.

Materials and Methods

Purification of Hsp70, Hsp90, Cp149, and HBV capsid assembly

Hsp70, Hsp90, and Cp149 were cloned directly into a pET28b vector (Novagen, Wisconsin, USA). All constructs were transformed into BL21(DE3) pLysS *Escherichia coli* cells (Novagen, Wisconsin, USA), and purified using HPLC columns (Gilson, Wisconsin, USA) and affinity chromatography with Ni-NTA resin. Proteins were stored in 10% glycerol at -20 °C. Capsid

assembly reactions were conducted in assembly reaction buffer (50 mM HEPES, 15 mM NaCl, 10 mM CaCl₂, pH 7.5). Samples with 20 μM Cp149 were incubated at 37 °C for 30 min. Assembled particles were detected using a 1% native agarose gel electrophoresis, and immunoblotting with anti-HBV antibodies (Abcam, Cambridge, UK) (Kim et al., 2015).

Co-immunoprecipitation of Hsp70 and Cp149, and sucrose density gradient

Twenty micromolar Cp149 in the form of dimers and capsids were mixed with 20 μM Hsp70, and incubated at 30 °C for 1 h for co-immunoprecipitation. A sucrose density gradient analysis was performed by ultracentrifugation (HITACHI, Tokyo, Japan) for 4 h at 4 °C, 250,000 *g*. Samples were treated with Hsp70 and 25 μM MB. Fractions from 1 to 11 (0-50% in steps of 5% sucrose concentration) (Kang et al., 2006), and co-immunoprecipitated samples were detected by 12% SDS-PAGE using the anti-HBV core (HBcAg) and Hsp70 antibodies (Santacruz, Texas, USA) (Shim et al., 2011).

Interaction analysis of proteins using microscale thermophoresis

Microscale thermophoresis was used to determine interactions between core protein and Hsps. Hsp70 and Hsp90 were fluorescence-labeled using a Monolith NT.115 protein labeling kit RED (Nanotemper, Munich, Germany), and were diluted to 20 μM in MST buffer, composed of 50 mM Tris-HCl (pH 7.4), 150 mM NaCl, 10 mM MgCl₂, and 0.05% Tween-20. The labeled

protein solutions were then incubated with serial concentrations of Cp149 dimer, capsid, and Hsp70, respectively. Also, solutions of labeled Hsp70 or Hsp90, incubated beforehand with Cp149 (Hsp-Cp149), were subsequently incubated with serial concentration of the other Hsp for thermophoresis analysis. Finally, serial concentration of Hsp90 with 25 μ M geldanamycin (GA) was examined for interaction with Cp149 and Hsp70-Cp149. All samples were incubated at 37 °C for 10 minutes. Thermophoresis parameters including molecule size, charge, and hydration shell were affected upon binding. Thermophoresis in a temperature gradient along the capillary was measured and analyzed using a non-linear curve fit with the Monolith NT.115 software (Nanotemper, Munich, Germany) (Timofeeva et al., 2012; Wienken et al., 2010).

Quantification of HBV DNA, RNA, and intracellular viral capsid

HepG2.2.15 cells were cultured in Dulbecco's modified Eagle's medium (DMEM, Wellgene, Gyeongsan-si, South Korea) with 10% fetal bovine serum (FBS) until 80% confluency. Then, cells were treated with MB (25 μ M) and GA (2.5 μ M) (Taiyab et al., 2009; Wang et al., 2010). A total of 150 nM of NC-siRNA and Hsp70-siRNA (Santacruz, Texas, USA) were transfected into HepG2.2.15 cells using the Fugene 6 transfection reagent (Roche, Basel, Swiss). After 24 h of incubation, extracellular viral DNA released into the medium was collected, and intracellular viral DNA was harvested from conjugated cells. Total RNA was isolated using the Ribozol RNA extraction reagent (Amresco, Ohio, USA), and cDNA was synthesized using a RT Drymix

(Enzynomics, Daejeon, South Korea). Total viral DNA and cDNA were quantified by performing a quantitative real-time PCR with SYBR-Green (Enzynomics, Daejeon, South Korea) (Cho et al., 2014). The forward primer sequence was 5'-TCCTCTTCATCCTGCTGCTATG-3', and reverse primer sequence was 5'-CGTGCTGGTAGTTGATGTTCCCT-3'. Intracellular HBV capsids from HepG2.2.15 cells were detected as described previously (Kim et al., 2015).

Synergistic analysis of capsid assembly

An *in vitro* HBV capsid assembly assay was performed with Hsp70 and Hsp90 in combinatorial concentrations (0, 2.5, 5, 7.5, 10, and 12.5 μ M). After 30 min at 37 °C incubation in the reaction buffer, samples were loaded on a 1% agarose gel, and assayed by immunoblotting. Each effect value was assessed by measuring the increase of the capsid assembly intensity in comparison with the control. Combination-index (CI) values were calculated using the Compusyn software (Molecular Pharmacology and Chemistry program, New York, USA). A dose-effect curve, CI-value plot, and isobologram plot were produced (Chou, 2006, 2010a).

Statistical analyses

Experimental data is presented as mean values \pm standard deviation from three independent experiments. Statistical analyses were performed using a Student's t-test. Fold change between

experimental and control groups is denoted on the bar graphs. Statistical significance was considered at $P < 0.05$.

Results

1. Hsp70 facilitates HBV core protein assembly into capsid

An *in vitro* capsid assembly assay with Hsp70 was performed, and the capsid formation of Cp149 increased correspondingly to an Hsp70 increase (Fig. 1A). Capsid assembly accelerated by Hsp70 decreased in the presence of MB (Fig. 1B). In order to confirm the effect of Hsp70 on the rate of HBV capsid assembly, changes in the intensity of capsid formation were measured at different reaction times. Capsid assembly was faster in the presence of Hsp70, compared to bovine serum albumin (BSA) or Hsp70 with MB (Fig. 1C). A sucrose density gradient analysis showed that Hsp70 increased the level of HBV capsid formation (Fig. 1D). BSA was used as a control.

2. Hsp70 shows synergistic effect with Hsp90 on capsid assembly

Capsid formation of Cp149 increased with increasing concentrations of Hsp70 and Hsp90 (Fig. 2A, 2B). Furthermore, capsid assembly synergistically increased with increasing concentrations of equivalently diluted Hsp70 and Hsp90 (Fig. 2C, Table 1). Synergistic effects on capsid formation by Hsp70 and Hsp90 were observed at 20 μM and 25 μM (concentrations of Hsp70 +

Hsp90). B23 (nucleophosmin) also increased HBV capsid assembly (Jeong et al., 2014). However, B23 and Hsp70 did not show synergistic effects on capsid assembly (Fig. 2D). Normalized capsid intensity results were plotted together (Fig. 2E). Increased capsid assembly in the presence of single Hsp70, Hsp90, and a combination of equivalent Hsp70 and Hsp90 proportions were plotted on a dose-effect curve. Effect values as functions of Hsp concentrations were analyzed with a logarithm curve fit (Fig. 2F). CI values at given Hsp concentrations were indicated on the combination index plot. CI values at 20 μ M and 25 μ M were below 1, indicating a synergistic effect (Fig. 2G). The isobologram showed that concentrations of Hsps are reduced in correspondence to synergistic effect (Fig. 2H) (Zhang et al., 2016). To examine whether each Hsp affected synergistic HBV capsid formation, we measured the capsid assembly at different concentration ratios of Hsp70 and Hsp90 (Fig. 3A, 3B). However, the dependency of synergistic effects on Hsp70 and Hsp90 produced no significant difference (Fig. 3C).

3. Hsp70 interacted with the HBV core protein dimer and Hsp90-core dimer complex

The thermophoresis results of Hsp70 and HBV Cp149 indicated that Hsp70 interacted with the Cp149 dimer (Fig. 4A), but not with the capsid (Fig. 4B). Hsp70 was predicted to interact with Cp149 dimer, but not with the capsid.

Thermophoresis was also measured for heat shock proteins (one labeled and previously

incubated with Cp149, and the other diluted in serial concentrations). Labeled Hsp90 with serial BSA concentration did not show a significant difference, whereas addition of serial Hsp70 concentration produced a concave thermophoresis curve (Figs. 4C and 4D). Similarly, Hsp90 showed a concave thermophoresis curve with labeled Hsp70, but not BSA (Figs. 4E and 4F). Labeled Hsp90 with serial Hsp70 (and vice versa) produced the dissociation constants $4.073 \pm 0.936 \mu\text{M}^{-1}$ and $4.755 \pm 2.299 \mu\text{M}^{-1}$, which was lower than the dissociation constants between heat shock proteins and Cp149 dimers (Table 2). It can be assumed that the alteration may be a consequence of a change in the equilibrium involving paired interactions between Hsp70, Hsp90, and Cp149. On the other hand, the both heat shock proteins may be able to bind to a complex between the other heat shock protein and Cp149 formed previously and build a complex of Hsp70, Hsp90, and Cp149.

The results of Hsp70 and Hsp90 indicated interactions between the two heat shock proteins in the capsid reaction condition (Fig. 4G). GA was observed to interact with Hsp90 (Fig. 4H). Upon GA addition, Hsp90 interacted with neither Cp149 nor Hsp70-Cp149 incubated in advance (Fig. 4I and 4J). The Hsp70 inhibitor MB was not used as it disturbed the fluorescence signal. Co-immunoprecipitation also showed Hsp70 binding to Cp149 dimers, but not to the capsid (Fig. 5A).

4. Inhibition of Hsp70 and Hsp90 reduces HBV replication in HepG2.2.15 cells

Intracellular and extracellular HBV DNA levels were quantified after knock-down or inhibition of Hsp70 and Hsp90 in HepG2.2.15 cells. Treatment with MB and knock-down of Hsp70 decreased the levels of intracellular and extracellular HBV DNA by 40%. Following treatment with both MB and GA, intracellular and extracellular HBV DNA levels were reduced by 70% (Fig. 5B). A knock-down effect of Hsp90 was reported in a previous study (Shim et al., 2011). We measured the expression level of HBV RNA; neither inhibition of Hsp70 nor of Hsp90 affected RNA expression levels (Fig. 5C). The results indicated that Hsp70 and Hsp90 are not involved in the transcription of cccDNA into HBV RNA. Intracellular capsid levels were measured by immunoblotting after inhibition. HepG2.2.15 cells were treated with MB and GA. Inhibition of Hsp70 or Hsp90 reduced intracellular capsid formation by 60% (Fig. 5D). Moreover, the capsid formation was reduced by 80% with MB and GA treatment together (Fig. 5D). However, the level of core protein was not affected by the Hsp70 and Hsp90 inhibitor treatment (Fig. 5D). These results demonstrated that inhibition of Hsp70 or Hsp90 interrupted the production of viral DNA by inhibiting capsid assembly.

Discussion

Drug compounds used in HBV therapy including lamivudine and adefovir target viral reverse transcriptase. However, long-term administration of these drugs induces drug resistance and results in reduced efficacy (Doong et al., 1991a). Although entecavir seem to produce less

drug resistance, study results are insufficient so far and other side effects have been reported (Pan et al., 2017). As an alternative solution for HBV therapy, newly developed drugs target HBV capsid formation (Dawood et al., 2017). Viral genome replication and virion maturation strongly depend on capsid assembly. Thus, capsid assembly has been suggested as a target for HBV therapy (Wu et al., 2013).

Several host factors are involved in virus infection and replication through interaction or encapsidating the polymerase and pgRNA during the HBV life cycle (Hu et al., 1997; Jeong et al., 2014). Among these host factors, the heat shock proteins exhibit various effects on HBV capsid formation. Hsp90 is known to facilitate capsid assembly and HBV particle production (Shim et al., 2011). In contrast, Hsp40 is reported to negatively affect capsid formation (Sohn et al., 2006).

In this study, we demonstrated that HBV capsid assembly increases after Hsp70 treatment, and Hsp70 and Hsp90 have a synergistic effect on capsid assembly *in vitro* (Fig. 1, 2, Table 1). We suggest that Hsp70 increases capsid assembly by catalyzing core protein hexamer formation, which acts as a nucleus in the capsid assembly. A BLAST analysis showed little protein sequence homology between Hsp70 and Hsp90 (Altschul et al., 1997). However, HBV capsid formation was increased by both heat shock proteins (Fig. 3) (Shim et al., 2011). These results indicate that Hsp70 and Hsp90 may simultaneously interact with core proteins and synergistically promote capsid formation (Fig. 2, 4). It is possible that multiple core protein

dimers interact with Hsp70 and Hsp90 in one complex. The formation of protein complexes of Cp149, Hsp70, and Hsp90 may be important for the understanding of synergistic effects of two heat shock proteins on capsid formation.

Although our results suggested a synergistic effect on capsid assembly through complex formation from Hsp70, Hsp90, and core protein (Fig. 2, 4), the effect of the two heat shock proteins on the HBV capsid assembly in a cellular environment remains unclear. Hsp70 and Hsp90 complexes involve cofactors when acting as molecular chaperones or regulating HBV polymerase activity (Pratt and Toft, 2003). Thus, further studies are needed to investigate each protein's capsid assembly promoting mechanism and the effect in *in vivo* systems, in order to better conclude on the effects of heat shock proteins on HBV viral capsid assembly.

Hsp70 has been suggested as a tumor prognosis marker recently and was reported to promote cancer growth. Thus, various cancer therapies were developed to target Hsp70 (Kumar et al., 2016). Particularly in hepatic tissue, expression of Hsp70 is known to promote oncogenesis, metastasis, and tumor cell invasion (Li et al., 2013). Cirrhosis and HCC are typically associated with an up-regulation of Hsp70 expression (Lim et al., 2005). Thus, the importance of Hsp70 in liver cancer is noteworthy not only as an HBV capsid assembly enhancer but also as an oncogenic factor in cancer-related pathological pathways.

The effect of Hsp70 as an enhancer and its synergistic effect with Hsp90 on HBV capsid assembly may give a novel insights for therapeutic strategies to treat chronic HBV

infections (Fig. 1, 2). Hsp70 and Hsp90 are involved in the HBV replication cycle and interact with the core protein, which makes them potential targets for HBV treatment associated with capsid assembly inhibition. In conclusion, understanding the functional effects of Hsp70 and Hsp90 on viral capsid assembly may contribute to the development of new HBV therapy drugs. Furthermore, it may shed light on correlations of Hsp70, Hsp90, chronic HBV infection, and HCC development.

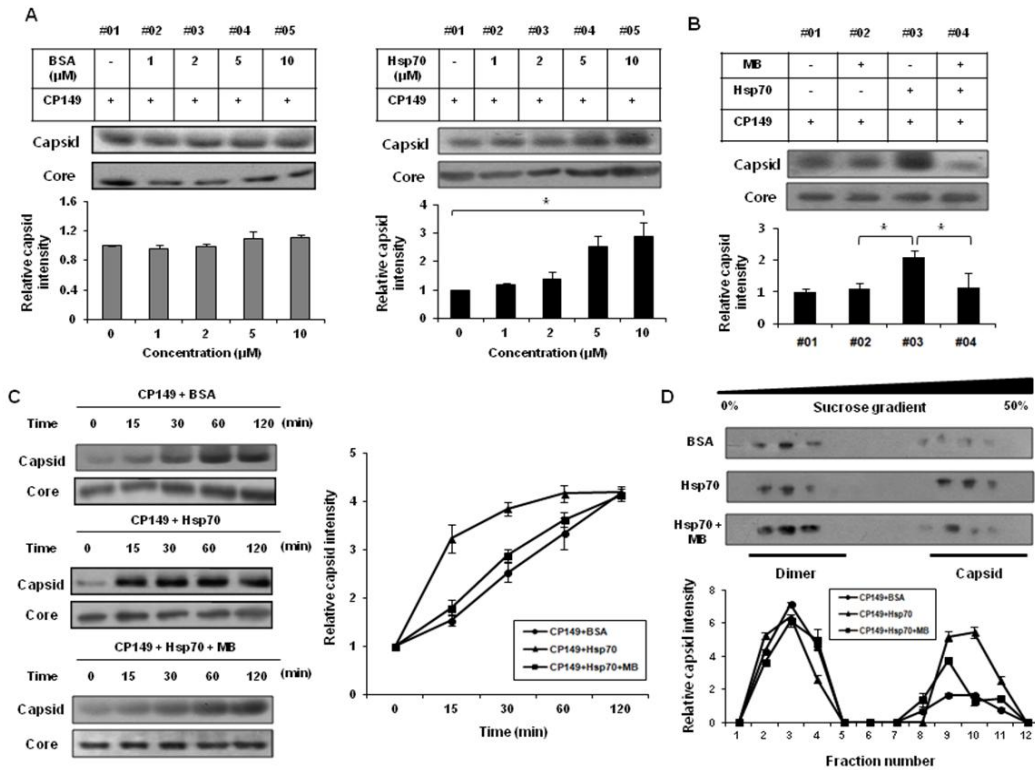


Fig. 1. Hsp70 promotes HBV core protein assembly.

A. BSA and Hsp70 concentration gradient (0, 1, 2, 5, 10 μM) to HBV capsid assembly. Capsid

intensity graph was plotted below. B. Inhibitor (25 μM MB) treated effect of Hsp70 on HBV

capsid assembly. C. Time gradient (0, 15, 30, 60, 120 min) of BSA (control), Hsp70, Hsp70+25

μM MB HBV capsid assembly. (MB = Methylene blue, BSA = Bovine serum albumin). All

samples were incubated in 37 $^{\circ}\text{C}$, reaction buffer. D. Sucrose density analysis of capsid assembly with BSA, Hsp70 and Hsp70+25 μM MB.

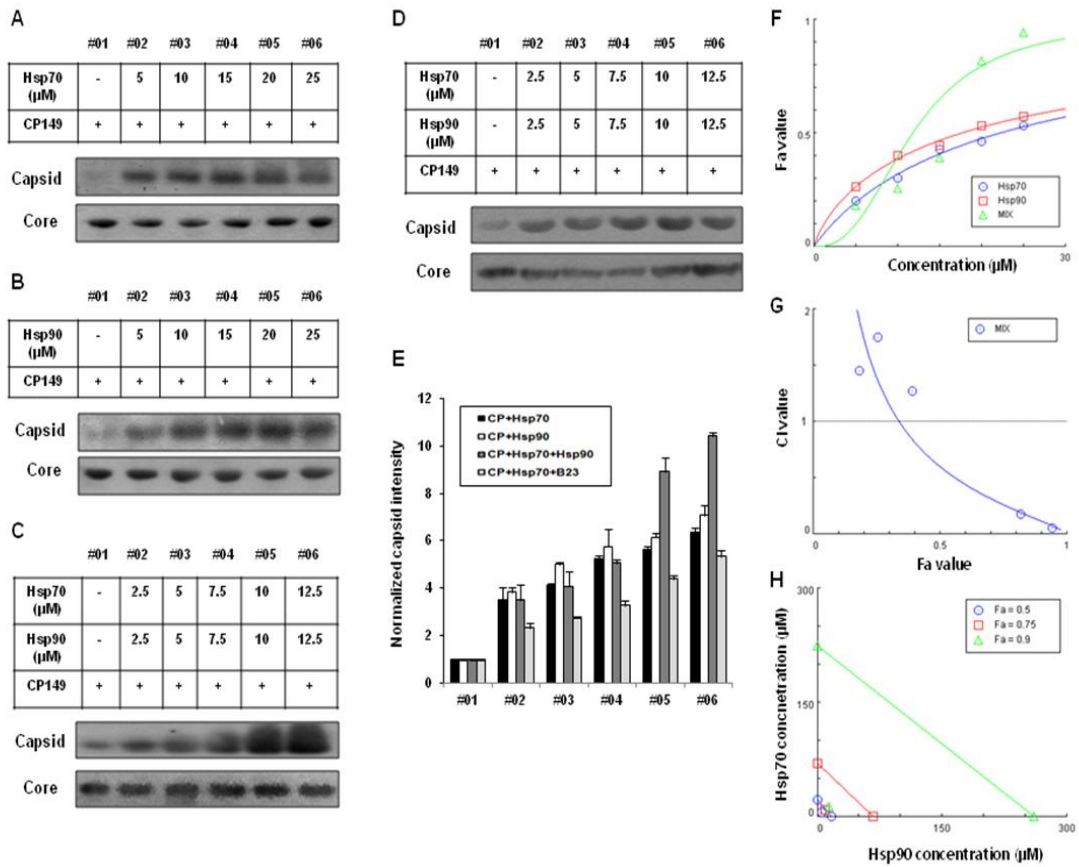


Fig. 2. Synergistic effect between Hsp70 and Hsp90 on HBV capsid assembly.

A-B. HBV capsid assembly by Hsp70/Hsp90 concentration gradient (5, 10, 15, 20, 25 μM). C. HBV capsid assembly with Hsp70 and Hsp90. D. HBV capsid assembly with Hsp70 and B23 (B23 = Nucleophosmin). E. Capsid assembly among Hsp70, Hsp90 and B23, normalized. F. Hsp70 and Hsp90 Dose-effect curve. G. Combination index (CI) plot. H. Isobologram plot.

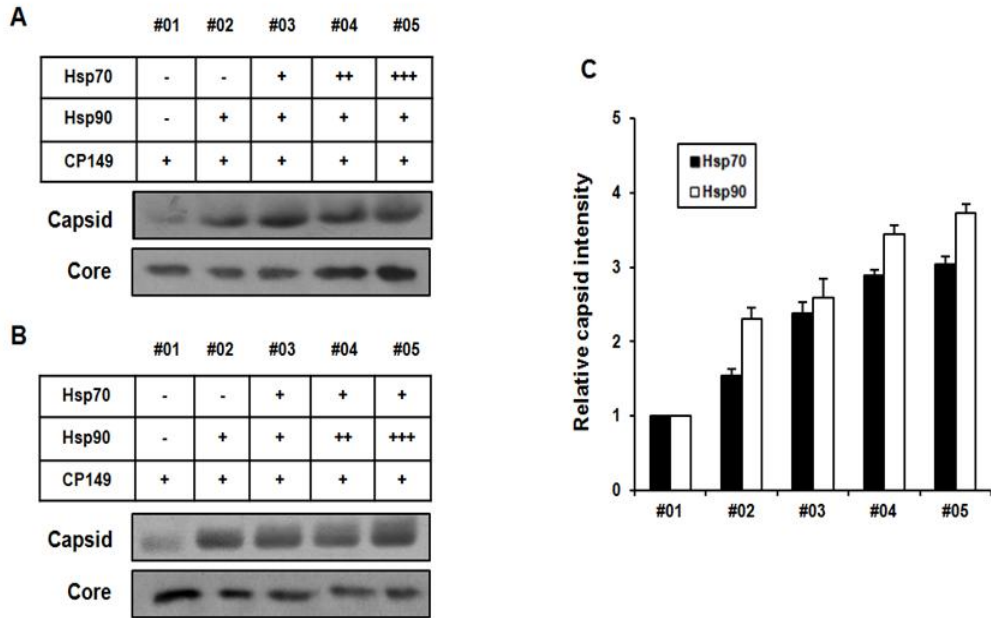


Fig. 3. Comparison of HBV capsid assembly increasing with Hsp70 or Hsp90.

A-B. HBV capsid assembly change by a gradient of the Hsp70/90 concentration (2.5, 5, and 7.5 μ M) and constant Hsp90 concentration (2.5 μ M). C. Relative capsid assembly intensity in gradient Hsp70 and Hsp90 treatment. The + sign indicates a 2.5 μ M concentration of Hsp70, Hsp90.

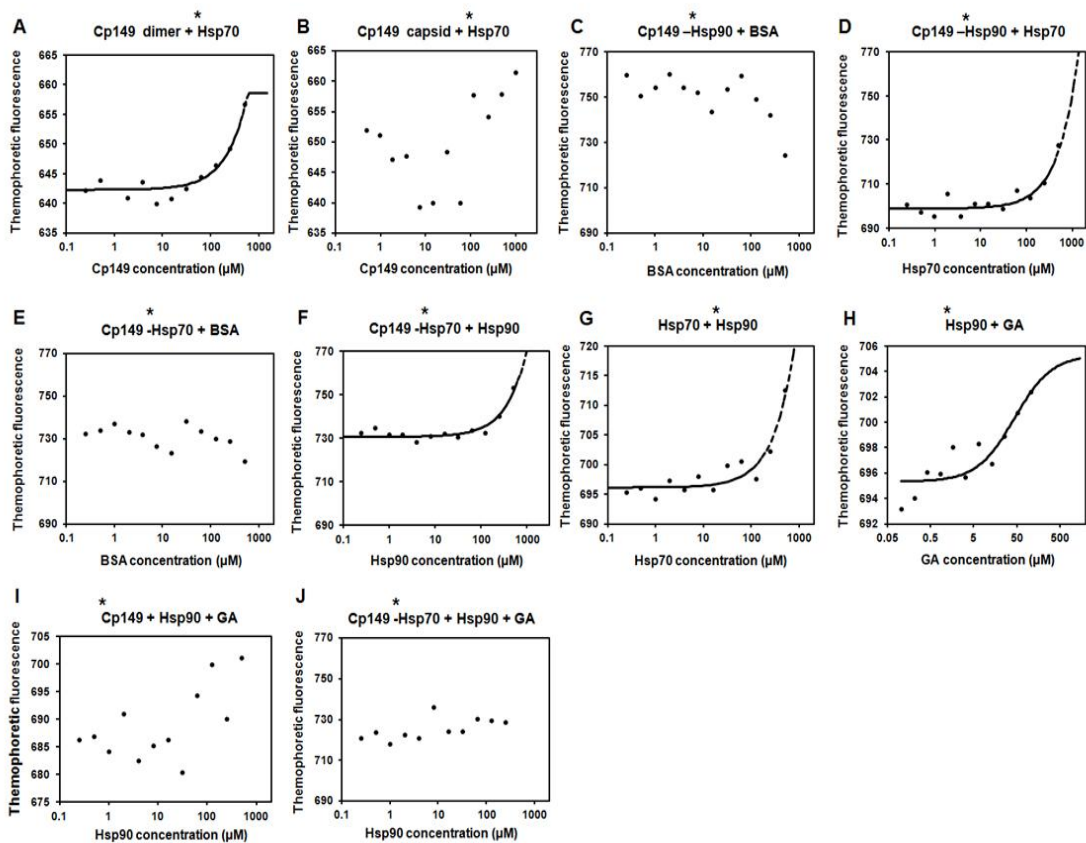


Fig. 4. Various combination of Thermophoresis analysis.

Microscale thermophoresis analysis between Hsp70, Hsp90, BSA, GA and Cp149.

A-B. Cp149 dimer/capsid and Hsp70 (labeled). C-D. Hsp90 (labeled)-Cp149 dimer reacted ahead and BSA/Hsp70. E-F. Hsp70 (labeled)-Cp149 dimer reacted ahead and BSA/Hsp90. G. Hsp70 and Hsp90 (labeled). H. Hsp90 (labeled) and GA. I. Cp149 dimer (labeled) and Hsp90 with GA treatment. J. Hsp70 (labeled)-Cp149 dimer reacted ahead and Hsp90 with GA treatment.

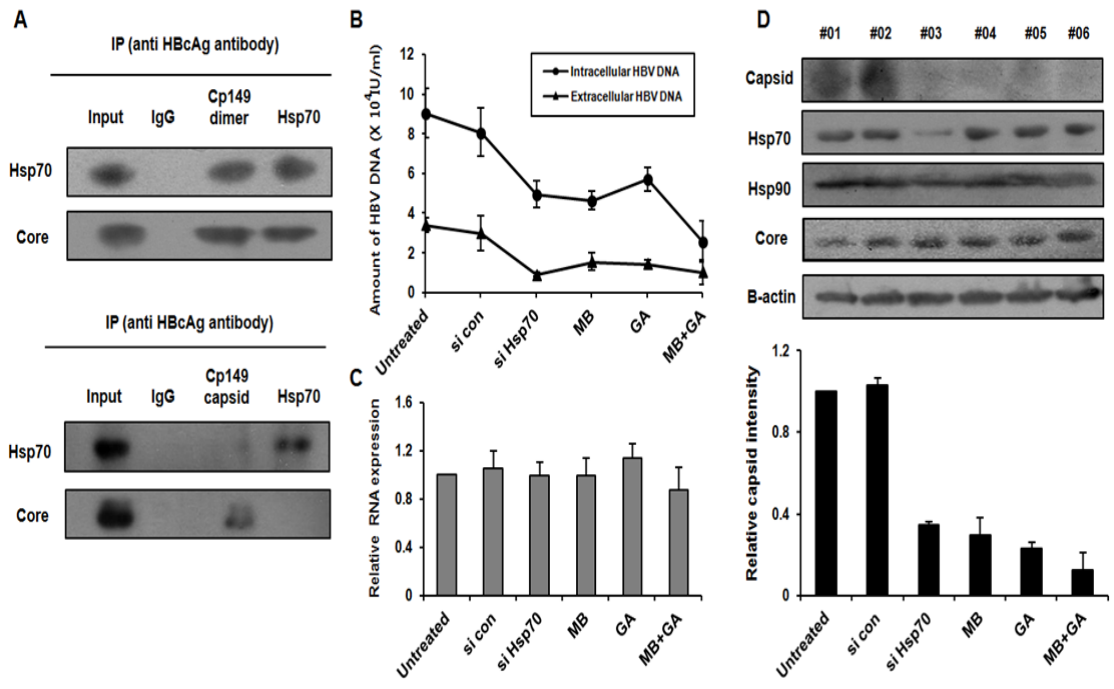


Fig. 5. Inhibition of Hsp70 and Hsp90 reduce HBV replication in HepG2.2.15 cells.

A. Co-immunoprecipitation (Co-IP) of Hsp70 with Cp149 dimer and capsid. B. Intracellular and extracellular HBV DNA titers. C. Relative RNA expression. D. Intracellular HBV capsid assembly immuno-blotting. Core protein, Hsp70, Hsp90 and β -actin were detected from HepG2.2.15 cells.

Table 1. CI values of Hsp70 and Hsp90 combinations on HBV capsid assembly (ratio 1 : 1).

Concentration ratio Hsp70 : Hsp90 (μ M)	Concentrations of Hsp70 + Hsp90 (μ M)	Fa value	CI value	Synergistic effect
2.5 : 2.5	5.0	0.182	2.900	---
5.0 : 5.0	10.0	0.256	3.497	----
7.5 : 7.5	15.0	0.391	2.549	---
10.0 : 10.0	20.0	0.819	0.361	+++
12.5 : 12.5	25.0	0.943	0.103	++++

All combination ratios are shown as (Hsp70 amount):(Hsp90 amount). CI values were calculated with compusyn software. CI value (Combination index) is an index that indicates synergism, additive effects, and antagonism.

Table 2. Kd values derived from Thermophoresis analysis.

Fluorescence labeled protein	Unlabeled protein		
	Cp149 dimer	Cp149 capsid	Incubated Cp149- different Hsp
BSA	-	-	-
Hsp70	9.957 ± 1.066 (μM^{-1})	-	4.755 ± 2.299 (μM^{-1})
Hsp90	5.244 ± 0.630 (μM^{-1})	-	4.073 ± 0.936 (μM^{-1})

A different Hsp indicates the other Hsp, Hsp70 for Hsp90, and vice versa. Kd values (dissociation constant) are shown as mean ± standard deviation.

Reference

- Alderson, T.R., Kim, J.H., Markley, J.L., 2016. Dynamical Structures of Hsp70 and Hsp70-Hsp40 Complexes. *Structure* 24, 1014-1030.
- Altschul, S.F., Madden, T.L., Schaffer, A.A., Zhang, J., Zhang, Z., Miller, W., Lipman, D.J., 1997. Gapped BLAST and PSI-BLAST: a new generation of protein database search programs. *Nucleic Acids Res* 25, 3389-3402.
- Argos, P., Fuller, S.D., 1988. A model for the hepatitis B virus core protein: prediction of antigenic sites and relationship to RNA virus capsid proteins. *EMBO J* 7, 819-824.
- Baaske, P., Wienken, C.J., Reineck, P., Duhr, S., Braun, D., 2010. Optical thermophoresis for quantifying the buffer dependence of aptamer binding. *Angew Chem Int Ed Engl* 49, 2238-2241.
- Bartenschlager, R., Schaller, H., 1992. Hepadnaviral assembly is initiated by polymerase binding to the encapsidation signal in the viral RNA genome. *EMBO J* 11, 3413-3420.
- Beasley, R.P., 1988. Hepatitis B virus. The major etiology of hepatocellular carcinoma. *Cancer* 61, 1942-1956.
- Beasley, R.P., Hwang, L.Y., Lin, C.C., Chien, C.S., 1981. Hepatocellular carcinoma and hepatitis B virus. A prospective study of 22 707 men in Taiwan. *Lancet* 2, 1129-1133.
- Birnbaum, F., Nassal, M., 1990. Hepatitis B virus nucleocapsid assembly: primary structure requirements in the core protein. *J Virol* 64, 3319-3330.
- Brunetto, M.R., Lok, A.S., 2010. New approaches to optimize treatment responses in chronic hepatitis B. *Antivir Ther* 15 Suppl 3, 61-68.
- Budkowska, A., Shih, J.W., Gerin, J.L., 1977. Immunochemistry and polypeptide composition of hepatitis B core antigen (HBc Ag). *J Immunol* 118, 1300-1305.

Buscher, M., Reiser, W., Will, H., Schaller, H., 1985. Transcripts and the putative RNA pregenome of duck hepatitis B virus: implications for reverse transcription. *Cell* 40, 717-724.

Chen, S., Prapapanich, V., Rimerman, R.A., Honore, B., Smith, D.F., 1996. Interactions of p60, a mediator of progesterone receptor assembly, with heat shock proteins hsp90 and hsp70. *Mol Endocrinol* 10, 682-693.

Chisari, F.V., Ferrari, C., 1995. Hepatitis B virus immunopathogenesis. *Annu Rev Immunol* 13, 29-60.

Cho, M.H., Jeong, H., Kim, Y.S., Kim, J.W., Jung, G., 2014. 2-amino-N-(2,6-dichloropyridin-3-yl)acetamide derivatives as a novel class of HBV capsid assembly inhibitor. *J Viral Hepat* 21, 843-852.

Cho, M.H., Song, J.S., Kim, H.J., Park, S.G., Jung, G., 2013. Structure-based design and biochemical evaluation of sulfanilamide derivatives as hepatitis B virus capsid assembly inhibitors. *J Enzyme Inhib Med Chem* 28, 916-925.

Chou, T.C., 2006. Theoretical basis, experimental design, and computerized simulation of synergism and antagonism in drug combination studies. *Pharmacol Rev* 58, 621-681.

Chou, T.C., 2010a. Drug combination studies and their synergy quantification using the Chou-Talalay method. *Cancer Res* 70, 440-446.

Chou, T.C., 2010b. Drug Combination Studies and Their Synergy Quantification Using the Chou-Talalay Method. *Cancer Res* 70, 440-446.

Crowther, R.A., Kiselev, N.A., Bottcher, B., Berriman, J.A., Borisova, G.P., Ose, V., Pumpens, P., 1994. Three-dimensional structure of hepatitis B virus core particles determined by electron cryomicroscopy. *Cell* 77, 943-950.

Dawood, A., Abdul Basit, S., Jayaraj, M., Gish, R.G., 2017. Drugs in Development for Hepatitis B. *Drugs* 77, 1263-1280.

Doong, S.L., Tsai, C.H., Schinazi, R.F., Liotta, D.C., Cheng, Y.C., 1991a. Inhibition of the Replication of Hepatitis-B Virus In vitro by 2',3'-Dideoxy-3'-Thiacytidine and Related Analogs. *Proceedings of the National Academy of Sciences of the United States of America* 88, 8495-8499.

Doong, S.L., Tsai, C.H., Schinazi, R.F., Liotta, D.C., Cheng, Y.C., 1991b. Inhibition of the replication of hepatitis B virus in vitro by 2',3'-dideoxy-3'-thiacytidine and related analogues. *Proc Natl Acad Sci U S A* 88, 8495-8499.

Fabrizi, F., Dulai, G., Dixit, V., Bunnapradist, S., Martin, P., 2004. Lamivudine for the treatment of hepatitis B virus-related liver disease after renal transplantation: meta-analysis of clinical trials. *Transplantation* 77, 859-864.

Flaherty, K.M., DeLuca-Flaherty, C., McKay, D.B., 1990. Three-dimensional structure of the ATPase fragment of a 70K heat-shock cognate protein. *Nature* 346, 623-628.

Gallina, A., Bonelli, F., Zentilin, L., Rindi, G., Muttini, M., Milanesi, G., 1989. A recombinant hepatitis B core antigen polypeptide with the protamine-like domain deleted self-assembles into capsid particles but fails to bind nucleic acids. *J Virol* 63, 4645-4652.

Ganem, D., Varmus, H.E., 1987. The molecular biology of the hepatitis B viruses. *Annu Rev Biochem* 56, 651-693.

Garson, J.A., Grant, P.R., Ayliffe, U., Ferns, R.B., Tedder, R.S., 2005. Real-time PCR quantitation of hepatitis B virus DNA using automated sample preparation and murine cytomegalovirus internal control. *J Virol Methods* 126, 207-213.

Grimm, D., Thimme, R., Blum, H.E., 2011. HBV life cycle and novel drug targets. *Hepatol Int* 5, 644-653.

Gust, I.D., Burrell, C.J., Coulepis, A.G., Robinson, W.S., Zuckerman, A.J., 1986. Taxonomic classification of human hepatitis B virus. *Intervirology* 25, 14-29.

Hirsch, R.C., Lavine, J.E., Chang, L.J., Varmus, H.E., Ganem, D., 1990. Polymerase gene products of hepatitis B viruses are required for genomic RNA packaging as well as for reverse transcription. *Nature* 344, 552-555.

Hu, J., Toft, D.O., Seeger, C., 1997. Hepadnavirus assembly and reverse transcription require a multi-component chaperone complex which is incorporated into nucleocapsids. *EMBO J* 16, 59-68.

Jeong, H., Cho, M.H., Park, S.G., Jung, G., 2014. Interaction between nucleophosmin and HBV core protein increases HBV capsid assembly. *FEBS Lett* 588, 851-858.

Kang, H.Y., Lee, S., Park, S.G., Yu, J., Kim, Y., Jung, G., 2006. Phosphorylation of hepatitis B virus Cp at Ser87 facilitates core assembly. *Biochem J* 398, 311-317.

Kim, Y.S., Seo, H.W., Jung, G., 2015. Reactive oxygen species promote heat shock protein 90-mediated HBV capsid assembly. *Biochem Biophys Res Commun* 457, 328-333.

Korba, B.E., 1996. In vitro evaluation of combination therapies against hepatitis B virus replication. *Antiviral Res* 29, 49-51.

Kumar, S., Stokes, J., 3rd, Singh, U.P., Scisum Gunn, K., Acharya, A., Manne, U., Mishra, M., 2016. Targeting Hsp70: A possible therapy for cancer. *Cancer Lett* 374, 156-166.

Lee, J.E., Lee, J.M., Lee, Y., Park, J.W., Suh, J.Y., Um, H.S., Kim, Y.G., 2017. The antiplaque and bleeding control effects of a cetylpyridinium chloride and tranexamic acid mouth rinse in patients with gingivitis. *J Periodontal Implant Sci* 47, 134-142.

Lee, M.J., Song, H.J., Jeong, J.Y., Park, S.Y., Sohn, U.D., 2013. Anti-Oxidative and Anti-

Inflammatory Effects of QGC in Cultured Feline Esophageal Epithelial Cells. *Korean J Physiol Pharmacol* 17, 81-87.

Lee, W.M., 1997. Hepatitis B virus infection. *N Engl J Med* 337, 1733-1745.

Li, H., Li, Y., Liu, D., Sun, H., Su, D., Yang, F., Liu, J., 2013. Extracellular HSP70/HSP70-PCs promote epithelial-mesenchymal transition of hepatocarcinoma cells. *PLoS One* 8, e84759.

Lim, S.O., Park, S.G., Yoo, J.H., Park, Y.M., Kim, H.J., Jang, K.T., Cho, J.W., Yoo, B.C., Jung, G.H., Park, C.K., 2005. Expression of heat shock proteins (HSP27, HSP60, HSP70, HSP90, GRP78, GRP94) in hepatitis B virus-related hepatocellular carcinomas and dysplastic nodules. *World J Gastroenterol* 11, 2072-2079.

Lott, L., Beames, B., Notvall, L., Lanford, R.E., 2000. Interaction between hepatitis B virus core protein and reverse transcriptase. *J Virol* 74, 11479-11489.

Mager, W.H., Ferreira, P.M., 1993. Stress response of yeast. *Biochem J* 290 (Pt 1), 1-13.

Mathew, A., Morimoto, R.I., 1998. Role of the heat-shock response in the life and death of proteins. *Ann N Y Acad Sci* 851, 99-111.

Mutimer, D., Pillay, D., Cook, P., Ratcliffe, D., O'Donnell, K., Dowling, D., Shaw, J., Elias, E., Cane, P.A., 2000. Selection of multiresistant hepatitis B virus during sequential nucleoside-analogue therapy. *J Infect Dis* 181, 713-716.

Nahleh, Z., Tfayli, A., Najm, A., El Sayed, A., Nahle, Z., 2012. Heat shock proteins in cancer: targeting the 'chaperones'. *Future Med Chem* 4, 927-935.

Ott, J.J., Stevens, G.A., Groeger, J., Wiersma, S.T., 2012. Global epidemiology of hepatitis B virus infection: new estimates of age-specific HBsAg seroprevalence and endemicity. *Vaccine* 30, 2212-2219.

Pan, H.Y., Pan, H.Y., Song, W.Y., Zheng, W., Tong, Y.X., Yang, D.H., Dai, Y.N., Chen, M.J., Wang, M.S., Huang, Y.C., Zhang, J.J., Huang, H.J., 2017. Long-term outcome of telbivudine versus entecavir in treating higher viral load chronic hepatitis B patients without cirrhosis. *J Viral Hepat* 24 Suppl 1, 29-35.

Paradis, V., 2013. Histopathology of hepatocellular carcinoma. *Recent Results Cancer Res* 190, 21-32.

Popkin, D.L., Zilka, S., Dimaano, M., Fujioka, H., Rackley, C., Salata, R., Griffith, A., Mukherjee, P.K., Ghannoum, M.A., Esper, F., 2017. Cetylpyridinium Chloride (CPC) Exhibits Potent, Rapid Activity Against Influenza Viruses in vitro and in vivo. *Pathog Immun* 2, 252-269.

Pratt, W.B., 1997. The role of the hsp90-based chaperone system in signal transduction by nuclear receptors and receptors signaling via MAP kinase. *Annu Rev Pharmacol Toxicol* 37, 297-326.

Pratt, W.B., Toft, D.O., 2003. Regulation of signaling protein function and trafficking by the hsp90/hsp70-based chaperone machinery. *Exp Biol Med (Maywood)* 228, 111-133.

Ren, Q., Liu, X., Luo, Z., Li, J., Wang, C., Goldmann, S., Zhang, J., Zhang, Y., 2017. Discovery of hepatitis B virus capsid assembly inhibitors leading to a heteroaryldihydropyrimidine based clinical candidate (GLS4). *Bioorg Med Chem* 25, 1042-1056.

Seeger, C., Mason, W.S., 2000. Hepatitis B virus biology. *Microbiol Mol Biol Rev* 64, 51-68.

Selzer, L., Katen, S.P., Zlotnick, A., 2014. The hepatitis B virus core protein intradimer interface modulates capsid assembly and stability. *Biochemistry* 53, 5496-5504.

Shim, H.Y., Quan, X., Yi, Y.S., Jung, G., 2011. Heat shock protein 90 facilitates formation of the HBV capsid via interacting with the HBV core protein dimers. *Virology* 410, 161-169.

Smith, J.R., Evans, K.J., Wright, A., Willows, R.D., Jamie, J.F., Griffith, R., 2012. Novel indoleamine 2,3-dioxygenase-1 inhibitors from a multistep in silico screen. *Bioorg Med Chem* 20, 1354-1363.

Sohn, S.Y., Kim, S.B., Kim, J., Ahn, B.Y., 2006. Negative regulation of hepatitis B virus replication by cellular Hsp40/DnaJ proteins through destabilization of viral core and X proteins. *J Gen Virol* 87, 1883-1891.

Stein, L.L., Loomba, R., 2009. Drug targets in hepatitis B virus infection. *Infect Disord Drug Targets* 9, 105-116.

Summers, J., 1988. The replication cycle of hepatitis B viruses. *Cancer* 61, 1957-1962.

Summers, J., Mason, W.S., 1982. Replication of the genome of a hepatitis B--like virus by reverse transcription of an RNA intermediate. *Cell* 29, 403-415.

Taiyab, A., Sreedhar, A.S., Rao Ch, M., 2009. Hsp90 inhibitors, GA and 17AAG, lead to ER stress-induced apoptosis in rat histiocytoma. *Biochem Pharmacol* 78, 142-152.

Timofeeva, O.A., Chasovskikh, S., Lonskaya, I., Tarasova, N.I., Khavrutskii, L., Tarasov, S.G., Zhang, X., Korostyshevskiy, V.R., Cheema, A., Zhang, L., Dakshanamurthy, S., Brown, M.L., Dritschilo, A., 2012. Mechanisms of unphosphorylated STAT3 transcription factor binding to DNA. *J Biol Chem* 287, 14192-14200.

Vanlandschoot, P., Cao, T., Leroux-Roels, G., 2003. The nucleocapsid of the hepatitis B virus: a remarkable immunogenic structure. *Antiviral Res* 60, 67-74.

Waite, N.M., Thomson, L.G., Goldstein, M.B., 1995. Successful vaccination with intradermal hepatitis B vaccine in hemodialysis patients previously nonresponsive to intramuscular hepatitis B vaccine. *J Am Soc Nephrol* 5, 1930-1934.

Wang, A.M., Morishima, Y., Clapp, K.M., Peng, H.M., Pratt, W.B., Gestwicki, J.E., Osawa, Y., Lieberman, A.P., 2010. Inhibition of hsp70 by methylene blue affects signaling protein function and ubiquitination and modulates polyglutamine protein degradation. *J Biol Chem* 285, 15714-15723.

Whitley, D., Goldberg, S.P., Jordan, W.D., 1999. Heat shock proteins: a review of the molecular chaperones. *J Vasc Surg* 29, 748-751.

Wienken, C.J., Baaske, P., Rothbauer, U., Braun, D., Duhr, S., 2010. Protein-binding assays in biological liquids using microscale thermophoresis. *Nat Commun* 1, 100.

Wolters, L.M., Niesters, H.G., de Man, R.A., 2001. Nucleoside analogues for chronic hepatitis B. *Eur J Gastroenterol Hepatol* 13, 1499-1506.

Wu, G., Liu, B., Zhang, Y., Li, J., Arzumanyan, A., Clayton, M.M., Schinazi, R.F., Wang, Z., Goldmann, S., Ren, Q., Zhang, F., Feitelson, M.A., 2013. Preclinical characterization of GLS4, an inhibitor of hepatitis B virus core particle assembly. *Antimicrob Agents Chemother* 57, 5344-5354.

Wynne, S.A., Crowther, R.A., Leslie, A.G., 1999. The crystal structure of the human hepatitis B virus capsid. *Mol Cell* 3, 771-780.

Yang, L., Lu, M., 2017. Small molecule inhibitors of hepatitis B virus nucleocapsid assembly: a new approach to treat chronic HBV infection. *Curr Med Chem*.

Young, J.C., Moarefi, I., Hartl, F.U., 2001. Hsp90: a specialized but essential protein-folding tool. *J Cell Biol* 154, 267-273.

Zhang, N., Fu, J.N., Chou, T.C., 2016. Synergistic combination of microtubule targeting anticancer fludelson with cytoprotective panaxytriol derived from panax ginseng against MX-1 cells in vitro: experimental design and data analysis using the combination index method. *Am J Cancer Res* 6, 97-104.

Zlotnick, A., Ceres, P., Singh, S., Johnson, J.M., 2002. A small molecule inhibits and misdirects assembly of hepatitis B virus capsids. *J Virol* 76, 4848-4854.

Zuckerman, A.J., 1999a. More than third of world's population has been infected with hepatitis B virus. *British Medical Journal* 318, 1213-1213.

Zuckerman, A.J., 1999b. More than third of world's population has been infected with hepatitis B virus. *BMJ* 318, 1213.

국문초록

B형간염 바이러스 감염은 전세계적으로 만성간질환, 간염, 간암을 일으키는 위험요소중의 하나이다. 다양한 B형간염 바이러스 관련 약물들이 개발되었으나, 약물에 대한 내성 및 약한 효율성에 대한 부작용으로 활용성에 한계점이 존재한다. 그러므로 이를 대체할 만한 B형간염 바이러스 환자 개개인에 대한 약물의 개발이 시급한 실정이다. 우리는 염화세틸피리디늄을 중요한 B형간염 바이러스 억제제로 발견하였다. 컴퓨터를 이용한 도킹모델링과 Microscale thermophoresis 분석, *in vitro* 캡시드형성 assay를 통해서 우리는 염화세틸피리디늄이 코어단백질 이합체와 결합함을 확인하였다. 벤젠설폰아마이드, 설파닐아민 등의 다른 B형간염 바이러스 억제제와의 비교를 통해서 염화세틸피리디늄은 인간 간암세포주로서 B형간염 바이러스를 분비하는 HepG2.2.15 세포에서 바이러스 수를 상당히 감소시킴을 확인하였다. 또한 마우스 동물실험에서도 염화세틸피리디늄이 바이러스 복제를 억제시킴을 확인하였다. 우리의 결과는 염화세틸피리디늄이 B형간염 바이러스의 캡시드형성을 억제하고 바이러스 생성을 감소시킴을 밝혀냈으며, 나아가 염화세틸피리디늄이 B형간염 바이러스를 감소시키는 효과적인 약학적 물질이라는 것을 증명해 준다.

또 다른 발견으로 열충격단백질은 B형간염 바이러스의 생활사에서 캡시드형성과 유전

자복제에 중요한 역할을 한다. 열충격단백질90은 B형간염 바이러스 캡시드형성을 증가시킨다고 알려져 있다. 그러나 열충격단백질70과 90에 의한 캡시드형성에 대한 기능적인 역할은 연구가 되어있지 않다. Microscale thermophoresis와 In vitro 캡시드형성 assay를 통하여 우리는 열충격단백질70이 B형간염 바이러스 코어단백질 이합체와 결합하여 캡시드형성을 촉진시킨다는 것을 발견하였다. 메틸렌블루에 의한 열충격단백질70의 억제 는 B형간염바이러스 캡시드형성을 감소시켰으며, 나아가 이는 HepG2.2.15 세포에서 세포내의 캡시드형성과 바이러스수를 감소시킴을 확인하였다. 더욱이 우리는 열충격단백질 70과 90의 협동적효과에 의한 B형간염 바이러스 캡시드형성의 증가 또한 확인하였다. 우리의 결과는 열충격단백질70이 B형간염 바이러스 코어 단백질 이합체와 결합하여 캡시드형성을 증가시키고, 열충격단백질90과 함께 협동적으로 캡시드형성을 증가시키는 기능 등을 밝혀내었다.